



1 **Standardized field methods for fracture-focused surface processes**

2 **research**

3 Martha Cary Eppes¹, Jennifer Aldred², Samantha Berberich¹, Maxwell P. Dahlquist³, Sarah G. Evans⁴,
4 Russell Keanini⁵, Faye Moser¹, Mehdi Morovati⁵, Steven Porson¹, Monica Rasmussen¹, Alex Rinehart⁶, Uri
5 Shaanan⁷

6 ¹ Department of Geography & Earth Sciences, University of North Carolina at Charlotte, Charlotte, NC 28223, USA

7 ² New Mexico Highlands University, Las Vegas, NM, USA

8 ³ Department of Geology, University of the South, Sewanee, TN 37383, USA

9 ⁴ Department of Geological and Environmental Sciences, Appalachian State University, Boone, NC, 28608, USA

10 ⁵ Department of Mechanical Engineering and Engineering Science, University of North Carolina at Charlotte, Charlotte, NC
11 28223, USA

12 ⁶ Department of Earth and Environmental Sciences, New Mexico Institute of Mining and Technology, Socorro, NM, 87801,
13 USA

14 ⁷ Geological Survey of Israel, Jerusalem 9692100, Israel

15 *Correspondence to:* meppes@uncc.edu

16



Abstract. Rock fracturing comprises a key component of a broad array of Earth surface processes due to its direct control on rock strength as well as rock porosity and permeability. However, to date, there has been no standardization for the quantification of rock fractures in surface processes research. In this work, we make the case for standardization within fracture-focused research and review prior work to identify various key datasets and methodologies. We then present a suite of standardized methods that we propose as ‘baseline’ for fracture-based research in surfaces processes studies. These methods have been shown in preexisting work from structural geology, fracture mechanics, and surface processes disciplines to comprise best practices for the characterization for cracks, clasts, and outcrops. These practical, accessible and detailed methods can readily be employed across all fracture-focused weathering and geomorphology applications. The wide adoption of a baseline of data, all collected using the same methods, will enable comparison and compilation of data among studies globally, and ultimately will lead to a better understanding of the links and feedbacks between rock fracture and landscape evolution.

1 Introduction

Rock fracture in surface and near-surface environments plays a key role in virtually all Earth surface processes. The propagation of opening-mode cracks (versus shear- or compression-mode) in bedrock and loose clasts occurs universally at or near the surface of Earth (e.g. within ~500 m - Moon et al., 2020) and on other terrestrial bodies (Molaro et al., 2020). It epitomizes mechanical weathering and the development of ‘critical zone architecture’, i.e., the evolving porosity, permeability, and strength of near-surface rock (e.g., Riebe et al., 2021). Herein, we use the terms crack and fracture interchangeably to refer to any planar, *open* void in rock, regardless of origin or scale (more details below), acknowledging that a large body of geologic literature also refers to veins or dikes - filled with secondary minerals - as ‘fractures’. The size, number, and/or orientation of fractures exert enormous influence on both rock mechanical properties (Ayatollahi and Akbardoost, 2014) and rock hydrological properties (e.g., Leone et al., 2020; Snowdon et al., 2021). Fractures therefore influence a wide array of natural and anthropogenic landscape features and processes including channel incision (e.g., Shobe et al., 2017), sediment size and production (e.g., Sousa, 2010), hillslope erosion (e.g., DiBiase et al., 2018; Neely et al., 2019), built environment degradation (Hatir, 2020), landslide and rockfall hazards (e.g., Collins and Stock, 2016), groundwater and surface water processes (e.g., Maffucci et al., 2015; Wohl, 2008), and vegetation distribution (e.g., Aich and Gross, 2008). Additionally, crack propagation and coalescence produce clastic sediment. The resultant physical properties of that sediment (i.e., clast size distribution, mass, porosity, etc.) control both hillslope and stream processes (e.g., Chilton and Spotila, 2020; Glade et al., 2019).

With fractures so clearly central to so many surface processes, it is crucial to understand the factors that control rock fracturing rates and processes. To fully do so requires a large body of data quantifying fracture-related characteristics and phenomena in a variety of subaerial environments; however, to date, no standardized set of field methods has been established to quantify cracks in the modern surface processes realm. Consequently, data collected across studies cannot be readily compared or coalesced. The purpose of this paper is therefore to define such standards for surface processes research by combining prior fracture methodology studies from other geoscience disciplines with methods that have been developed, tested and refined during more than 20 years of field-based crack-observations for surface processes-related research (Aldred et al., 2015; Eppes and Griffing, 2010; Eppes et al., 2018; Eppes et al., 2010; McFadden et al., 2005; Moser, 2017; Shobe et al., 2017; Weiserbs, 2017).

Building on this combination of past work, here, we first define the benefits of establishing a standard procedure for fracture-focused surface processes field research, describing how our chosen methods outperform other approaches. We then provide the



methods themselves including: 1) a set of guiding principles that should be employed for all surface processes research involving rock fractures; 2) a list of crack and rock data measurements that constitute “basic” field-based metrics; and 3) detailed methods that comprise best practices for collection of these data. Finally, we provide some suggestions for data analyses, and demonstrate a real case example of how the proposed methods lead to reproducible results across users. We limit ourselves to field observations on subaerially exposed rock, i.e., cracks that can be observed with the naked eye or basic hand lens on exposed outcrops or clasts. We do not address measurement of smaller cracks (e.g., those visible with microscopy) or of buried fractures (e.g., those visualized in bore-holes or with indirect geophysical methods). In providing these standardized methods to the surfaces processes community, we hope to accelerate the overall characterization and conceptualization of how a most basic feature of all rock – its open fractures – contributes to the processes and evolution of Earth’s surface and critical zone.

1.1 The value of a standardized approach

Particularly within the fields of geomorphology and weathering sciences, no common suite of data, methods, or terminology has been defined or described that comprises an analysis of fractures. Although some crack characterization field methods exist in the context of structural geology and aquifer and reservoir characterization (e.g., Watkins et al., 2015; Wu and Pollard, 1995; Zeeb et al., 2013), they diverge significantly in their approaches because they were largely developed for the specific application of each unique study. Furthermore, the terminology and methods used to describe natural fractures across this existing research are largely limited to only those fractures loosely interpreted to be tectonically induced ‘joints’, and published works rarely provide clear criteria, even for choosing which fractures to measure. This lack of consistency severely limits the ability of the geomorphic community to reproduce methods, or to combine, compare, or interpret different fracture datasets.

The dearth of standardized methodology in quantifying natural fractures is in contrast with methods available for other components of Earth systems. The development of consistent methods undergirds most quantitative Earth sciences. For example, the fields of sedimentology and soil science have clear, standardized methods to acquire what constitutes the “basic” data for their observations. Sedimentologists have long shared common metrics and methods for quantifying grain size, sorting, rounding, and stratigraphic records (e.g., Krumbein, 1943). Similarly, soil scientists share common methods, metrics, and nomenclature for describing soil profiles and horizons (e.g., Birkeland, 1999 Appendix A; Soil Survey Staff, 1999). The realization of the need for standard methods has also remained constant in lab based rock mechanics over the last several decades, driving the American Society for Testing and Materials (ASTM) and International Society for Rock Mechanics (ISMR) to publish ongoing standards and methods papers (e.g., Ulusay and Hudson, 2007).

Standards like those mentioned above exist because workers have long recognized and reaped the the benefits of standardized methods. Standardized methods can frequently lead to major step-change innovations when data are combined. For example, standardized soil methods allowed for 100 m scale mapping across the US, enabling detailed human–landscape models that can aid in preserving vital soil resources (Ramcharan et al., 2018). Another major example arises from the field of rock mechanics. Prior to the 1950s, theoretical developments of rock failure and plasticity lagged behind other branches of geophysics and engineering, limited both by technology and, arguably more so, by lack of consistent methods. Across rock mechanics, methods for repeatable failure testing were then developed, largely in the groups led by Knoppf, Griggs, and Turner in the USA and Australia (Wenk, 1979). This standardization culminated in the landmark series of papers that made the observations driving the next 50 years of experimental rock mechanics (Borg and Handin, 1966; Handin et al., 1963; Handin and Hager, 1958, 1957; Heard, 1963;



Mogi, 1971, 1967; Turner et al., 1954), as well as continued methods development in field and laboratory methods linking structural geology and experimental rock mechanics (Wenk, 1979).

Across the limited studies where field observation crack methods have been standardized, major advances have also occurred as a result. For example, noting the similarity of crack data collected with standardized methods across a range of climates (McFadden et al., 2005; Eppes et al., 2010; Eppes et al., 2015; Aldred et al., 2016) was foundational in motivating and validating the construction of a predictive model of how and why moisture impacts rates of crack evolution (e.g., Eppes and Keanini, 2017). This work has led to a greater appreciation within surface processes research that rock cracking is a complex, time- and climate-dependent, non-linear process. **How can we begin to understand it across teams without a standard set of observation methods?**

1.2 Development of the Standardized Crack Measurement Approach

Particularly for the case of fracture-focused research outside of geomorphology applications, the need for standardized methods has already been established. Within this prior body of research, the methods we propose below have been shown to outperform other approaches. In one case example, study participants were asked to measure fractures with no particular instructions given for how to collect the data other than where to collect it. The wide variance in resulting datasets collected by different users led to the conclusion that, without common and clearly established measurement criteria, fracture characterization is rife with subjective bias that severely impacts interpretations of results (Andrews et al., 2019). Then, based on post-data collection interviews and workshops, Andrews et al., (2019) scrutinized the source of the variance and provided a list of suggested best-practices that would serve to best eliminate the subjectivity of data collection that was leading to the bias.

In another case example, Zeeb et al. (2013) sought to determine how different sampling approaches leads to censoring bias of different crack sizes from outcrop data by applying different sampling methods to artificially generated fracture networks that had known parameters. Analysis of data collected using scanline, window, and circular estimator methods revealed that the window approach resulted in the lowest uncertainty for most parameters and required the fewest measurements to provide representative datasets.

We incorporate the suggested best-practices from the two case examples above as well as from other published research in the methods we describe below. For example, our approach of measuring any continuous open fracture as a single fracture is preferable over trying to interpret separate linked fractures, which can vary significantly depending on the scale of observation (e.g., Ortega and Marrett, 2000), and thus tends to amplify selective bias of the user (Andrews et al., 2019). Similarly, the use of a crack size cut-off has been shown in other studies to be crucial to maintaining reproducibility of results (e.g., Ortega et al., 2006), and window sampling was chosen as it provides the most accurate representation of the rock mass (e.g., Zeeb et al., 2013), and results in the least user-variance in results (Andrews et al., 2019). Measuring fracture apertures with a crack-comparator (section 8.4.2) provides better constrained aperture-size distributions than other techniques, particularly for sub mm widths (e.g., Ortega et al., 2006). Several studies have shown that measuring all fractures – i.e., a complete inventory as described in section 4.2 – provides the most accurate representation of the full fracture characteristics of a rock body (e.g., Wu and Pollard, 1995).

The standardized methods below were also chosen by us to optimize data collection as it relates to modern geomorphology questions. We focus on open fractures found in surface outcrops and clasts because these fractures can represent both surface and subsurface fracture processes, and impact rock strength and hydrology. Other geoscience research frequently employs crack



characteristic data from natural rock exposures. Outcrop fracture measurements are commonly employed to explain lithofacies variability observed in subsurface wireline logs for hydrocarbon production (e.g., Milad and Slatt, 2019) and structural modeling (e.g., Hennings et al., 2000), or to validate shallow geophysical measurements inferred to reflect fracture density (e.g., Flinchum et al., 2018; Novitsky et al., 2018). A major distinction between geomorphology and weathering fracture-focused research compared to other fracture-based geosciences is the recognition and interest in environmentally-driven cracking (see section 2.2 below for examples). Fracture data from loose clasts can serve to isolate environmentally-driven processes like thermal stress cracking from those related to gravity or tectonics (e.g., McFadden et al., 2005; see section 2.3 below). Thus, we describe methods for both outcrop and clast data collection.

2 Standardized methods: Guiding principles

2.1 Natural rock cracking background

The design of any fracture-related study must arise from consideration of the general factors that influence how and if a rock will crack. Here, we provide a very brief overview of some key rock fracture mechanics concepts behind these factors. Eppes and Keanini (2017) and Eppes (2022) provide more detailed reviews of rock fracture processes in the context of surface processes.

Rocks fracture in response to the complex sum of all tectonic (e.g., Martel, 2006), topographic (e.g., St. Clair et al., 2015; Moon et al., 2020; Molnar, 2004), biological (e.g., Brantley et al., 2017), and environment-related (e.g., Matsuoka and Murton, 2008; Gischig et al., 2011) stresses they experience. Fracturing can occur when stresses exceed the failure criteria (i.e., rock's material strength). More commonly, however, because critical stresses are only rarely reached in nature, fractures can also propagate *subcritically* at stresses as low or lower than 10% of the rock's strength (see textbooks like Schultz, 2019; Atkinson, 1987).

Overall, subcritical **cracking** processes and rates are strongly dependent on stress magnitude, but they are *also* strongly influenced by the size of the fracture that is under stress, as well as the environmental conditions that impact crack tip bond breaking (see fracture mechanics textbooks like Anderson, 2005). Stresses applied to the rock body are concentrated at crack tips proportional to the length of the crack (a concept embodied by the term 'stress intensity'), effectively increasing the stresses experienced directly in that location. The environmental factors known to impact subcritical rock cracking -- in a manner separate from their influence on stresses -- include vapor pressure, temperature, and pore-water chemistry (Eppes and Keanini, 2017; Eppes et al., 2020; Brantut et al., 2013). Therefore, in the context of surface processes, climate matters twice for rock cracking: 1) as it contributes to the stresses that the rock experiences, and 2) as it contributes to the chemo-physical processes that break bonds at crack tips as they propagate.

Just as other common physical properties like tensile strength can be measured, rocks can be tested for their propensity to crack subcritically by the measurement of subcritical cracking parameters such as the subcritical cracking index (e.g., Paris and Erdogan, 1963). These parameters influence both the rate and the characteristics (e.g., crack density or length) of subcritical cracking in rock (e.g., Olson, 2004). In sum, natural rock cracking is not necessarily the singular, catastrophic event as it is typically portrayed; but rather may be a slowly evolving process that progresses over geologic time that is influenced by complex amalgamations and feedbacks between rock and fracture properties, as well as environmental, topographic, and tectonic factors.

2.2 Site selection and study design using a State Factor approach



Due to their influence on rock cracking as described above, all potential driving stresses and variations in crack environments must be considered in site selection and study design for any fracture-related research. We recommend employing the ‘State Factor’ approach (Jenny, 1941) that has been well-vetted in the weathering and soil science disciplines. Here, we assert that applying this soil science paradigm to fracture research is relevant because fracturing processes are influenced by each of these factors, just as are all other chemical processes acting on rock and soil. This is particularly true when the subcritical nature of rock fracture is considered (section 2.1). Thus, by employing a State Factor approach to fracture-based research, all factors that could contribute to fracture propagation styles and rates are considered and controlled for as much as possible within the aims and scope of the research for any given site. These ‘State Factors’ - long categorized as they relate to overall soil development, of which physical weathering is a component (e.g., Jenny, 1941) - are equally applicable to fractures alone: climate (cl, both regional climate and microclimate), organisms (o, flora and fauna), relief (r, topography at all scales), parent material (p, rock properties) and time (t, exposure age or exhumation rate). For rock fracture, tectonics (T) should be added to this list, making cl,o,r,p,t,T.

Hereafter, we employ the term ‘site’ to refer to a single location, of either a group of rock clasts or a group of outcrops, whereby all clasts or outcrops within the ‘site’ could be reasonably assumed to have experienced similar State Factors over their exposure history. For example, a site might comprise a single boulder bar on an alluvial fan surface or a single ridgeline with several outcrops. Once the specific State Factors, including the internal variability of each site, are identified for all the sites within a given field area, a series of sites can be selected whose State Factors are known and controlled for as much as possible. This enables a study of the influence of a single factor across the sites, i.e., fracture chronosequences, climosequences, toposequences, or lithosequences.

As outlined in the background above, for rock fracture, it is important to understand how each cl,o,r,p,t,T factor may contribute both to stresses that give rise to cracking, and/or to the molecular-scale processes that serve to subcritically break bonds at crack tips. Each has the potential to independently impact cracking rates, styles, and processes. In the following paragraphs, we briefly provide examples of how each of the State Factors may influence rock fracture.

2.2.1 Climate (cl)

Climate (cl) as a State Factor refers not just to regional mean annual precipitation or temperature, but also the local microclimate of a site, which may be influenced by site characteristics such as runoff or aspect. The presence of liquid water increases the efficacy of water-related stress-loading processes like those related to freezing (Girard et al., 2013) or chemical precipitation of salts or oxides (e.g., Buss et al., 2008; Ponti et al., 2021). Moisture – particularly vapor pressure – can also serve to accelerate rock cracking rates independent of any stress-loading (e.g., Eppes et al., 2020; Nara et al., 2017). Temperature cycling can produce thermal stresses (through differential expansion and contraction of both adjacent minerals as well as different portions of the rock mass; e.g., Ravaji et al., 2019), and also can influence rates and processes of crack-tip bond breaking (e.g., Dove, 1995).

2.2.2 Organisms (o)

Organisms (o) refers to both flora and fauna - everything from overlying vegetation and large animals to roots and microorganisms, all of which may provide a source of rock stress and/or may influence water availability or chemistry. These relationships can be complex and unexpected. For example, tree motion during wind, and root swelling during water uptake, both exert stresses on rock directly (Marshall et al., 2021). Organism density and type can impact rock water and air chemistry (Burghel et al., 2015), both of which may impact the rates and processes of subcritical cracking (e.g. review in Brantut et al., 2013).



207 2.2.3 Relief (*r*)

208 In the context of State Factors, *relief* (*r*) refers generically to all metrics related to topography including aspect, slope, and
 209 convexity. Topography impacts the manifestation of both gravitational stresses as well as tectonic stresses within the rock body
 210 (Molnar, 2004; Moon et al., 2020; Martel, 2006). The directional aspect of a particular outcrop or boulder face may also influence
 211 insolation and water retention, translating into differences in micro climate and vegetation, and thus weathering overall (e.g.,
 212 Burnett et al., 2008; West et al., 2014; McAuliffe et al., 2022) including fracturing (Persico et al., 2021).

213 2.2.4 Parent material (*p*)

214 The *parent material* (*p*) factor in the context of a fracture study refers not only to the specific rock type being fractured, but also
 215 to the size and shape of the clast or outcrop. For example, angular corners generally concentrate stresses more than rounded edges
 216 (Anderson, 2005). Also, clasts or outcrops of different sizes experience different magnitudes of thermal stresses related to diurnal
 217 heating and cooling (Molaro et al., 2017). In addition to rock shape or size, rock material properties directly influence the rates and
 218 styles of fracture propagation (Atkinson, 1987) due both to how they respond to stresses but also due to how they allow stresses to
 219 arise. For example, different minerals are characterized by different coefficients of thermal expansion. As a result, rocks with
 220 different mineral constituents will be more or less sensitive to thermal stresses than others depending on the contrasts between
 221 adjacent grains. There is significant variance in this and many other material properties within any given category of rock type,
 222 such as ‘granite’ or ‘sandstone’. Grain size, porosity, sedimentary features, and metamorphic fabrics all influence the rates and
 223 characteristics of fracture growth and susceptibility to different environmental stresses.

224 2.2.5 Time (*t*)

225 *Time* (*t*) likely plays a role in rock fracturing rates just as it does in chemical weathering, whereby outcrops found in slowly-eroding
 226 environments or clasts found on old surfaces may be subject to different cracking rates and processes (e.g., Mushkin et al., 2014).
 227 Over time, rock mechanical properties can also change as rocks weather (e.g., Cuccuru et al., 2012). Although the time factor has
 228 not been well-studied in the context of natural rock fracture, preliminary data suggest that it should be considered (Berberich, 2020;
 229 Rasmussen et al., 2021).

230 2.2.6 Tectonics (*T*)

231 Finally, in a fracture-related study, *tectonic* (*T*) setting must also be considered as a State Factor. Joint sets that have formed in the
 232 deep subsurface inevitably become exhumed and further increase in both number density (total cracks per area) and intensity (total
 233 crack length per area) as they approach the surface. Also, even very low magnitude tectonic stresses can translate to fracture
 234 propagation in very near-surface bedrock, especially when interacting with local topography (e.g., Martel, 2011; Moon et al.,
 235 2020).

236 2.3 Bedrock outcrops versus deposited clasts

237 The fracture characteristics of outcrops have long been employed as proxies for subsurface fracture networks, and there is a
 238 reasonably large body of literature addressing these relationships and their potential pitfalls (e.g., Ukar et al., 2019; Al-Fahmi et
 239 al., 2020; Sharifigaliuk et al., 2021). Overall, we emphasize that the researcher should be aware that for any outcrop of *in situ*
 240 bedrock, tectonic stresses are likely not the only cause of fractures observed there. Importantly, fractures of all scales that may
 241 have initiated in response to rock crystallization, diagenesis, or tectonic stresses in the subsurface continue to propagate and evolve
 242 in the near-surface and once exposed subaerially. Thus, topographic and environmental stresses have likely both contributed to



any subaerially observed fracture network. For example, a commonly employed criterion for identifying what are interpreted as tectonically formed joints is that there are ‘several in parallel’ (e.g., Ewan et al., 1983). Yet, environmental stresses also produce parallel fractures (e.g., Aldred et al., 2015; Eppes et al., 2010; Mcfadden et al., 2005), as do those related to the morphology of the eroding landscape (Leith et al., 2014).

For studies that aim to isolate fractures associated with environmental stresses, measurements from clasts may be more useful than outcrops. Clasts that have been transported by fluvial, glacial, or mass-wasting processes have experienced abrasion, and therefore it is highly likely that pre-existing superficial fractures have been removed. Thus, clasts may be more reasonably considered ‘fresh’ than an outcrop with an unknown exhumation history, allowing clearer linkages between environmental exposure and observed fractures. This idea of “resetting” fractures within clasts through transport is supported by data showing clasts of identical rock type that have experienced more transport (i.e., rounded river rocks) having higher strength than those found in, for example, recent talus slopes (Olsen et al., 2020).

3 Standardized method: Selecting the clasts, outcrops, or rock surface locations that will comprise the fracture observation area

Carefully selecting the rock surface area(s) on which fractures will be observed and measured within a site is equally as important as selecting the site or the fractures themselves. Hereafter, we employ the term ‘observation area’ to refer to the specific portion(s) of rock surface(s) for which cracks are being measured. Observation areas may comprise the entire exposed surface of individual clasts, outcrops, or portions of either (Fig. 1). In the following sections, instructions for selecting these observation areas in the field are provided.

3.1 Establishing outcrop or clast selection criteria

Before observation areas can be identified, outcrops or clasts must be selected. The first step of that selection process is to establish criteria for determining which outcrops or surface clasts within the site are acceptable for measurement. Similar to site selection, variability in c,l,o,r,p,t factors that may influence cracking (temperature, moisture availability, rock shape, and rock type) should be controlled for as much as possible.

In general, characteristics of the clasts or outcrops that might impact mechanical properties, moisture, or thermal stress-loading should be most heavily considered. The rock type properties that should be considered when developing selection criteria include not only heterogeneities like bedding or foliation, but also grain size and mineralogy, all of which can influence fracture rates and style characteristics. For example, perhaps only outcrops with no visible veins or dikes will be employed; or only outcrops greater than 1 m in height; or only north facing outcrop faces. In past work, for example, we have focused on upward facing surfaces of outcrops or large clasts (e.g., Berberich, 2020; Eppes et al., 2018).

For loose clasts, only clasts of a particular size or rock type might be employed for measurement. For example, we have found that below approximately 5 cm diameter in semi-arid and arid environments (Eppes et al., 2010), and 15 cm in more temperate environments with vegetation (Aldred et al., 2015), the long-term stability of the positioning of the clast on the surface becomes questionable.

3.2 Non-biased selection of clasts or outcrops for measurement



Once criteria are defined, clasts or outcrops meeting those criteria must be chosen for the fracture measurements. A procedure such as the well-vetted Wolman Pebble Count style transect (Wolman, 1954) should be employed to avoid sampling bias. For landforms with other geometries, a grid may be used instead of a transect line. In either case, a tape transect or net grid is laid out on the ground at each site, and the clast or outcrop closest to specified intervals on the tape (or at the points of the grid meeting the criteria) is selected (Fig. 1a). The interval or grid spacing should be adjusted to the overall size and abundance of clasts or outcrops found on the surface. If there are relatively few meeting the criteria at a site, all within the site (e.g., on a particular boulder bar or ridgeline) meeting the criteria can be measured.

A similar technique can be applied for selecting more sparsely spaced outcrops. For locations where outcrops are common and vegetation relatively sparse, a grid of a set dimension (e.g., 100 m) is overlain on aerial imagery, and the closest outcrop to each grid intersection meeting the outcrop criteria are selected (Watkins et al., 2015). In sites where outcrops are few, all outcrops might be employed. For areas where outcrops are not visible in aerial imagery, a measured or paced transect can be employed where the user walks along a bearing and chooses the closest outcrop meeting the selection criteria at each interval, e.g., 30 paces.

In all of the above, transect locations and orientations should be selected following consistent criteria and being mindful of the State Factors cl, o, r, p, t, T . For example, all transects or grids might be placed uniformly along backslopes with a certain upslope distance from the crest; or along the latitudinal center or crest of a landform. Alternatively, the transect might be orientated perpendicular or oblique to a paleo-flow direction so that it is not constrained only to bars or swales. The coordinates and bearing of all transects or grids should be recorded, enabling tracking and avoiding repetition.

3.3 Observation areas comprising the entire clast or outcrop surface

The observation area for small clasts and outcrops can be their entire exposed surface. When clasts or outcrops selected for measurements are less than ~50 cm in maximum dimension, we recommend making measurements on all cracks visible on the clast or outcrop exposed surface, without disturbing the rock. This non-disturbance practice is particularly crucial for maintaining Earth's geodiversity (Brilha et al., 2018) and preserving sites for future workers to revisit. Further, research examining acoustic emission localization of rocks naturally cracking found that the large majority of crack 'foci' were located in the upper hemispheres of boulders (Eppes et al., 2016). Thus, we assert that the potential insight gained by moving clasts does not warrant its damage to geoheritage.

3.4 Establishing 'windows' as the observation area for larger clasts and outcrops

When it is not feasible to measure every crack on an outcrop or clast (in our experience this becomes true for most outcrops or boulders greater than 50 cm maximum diameter), the observation area may comprise predetermined 'windows' (Fig. 1b). This window selection method for the area of observation has been demonstrated to result in the most accurate representation of fractures on an entire outcrop (e.g., Zeeb et al., 2013) and is the least affected by subjective bias (Andrews et al., 2019). These windows comprise representative decimeter- to meter-scale square or rectangular areas of the rock surface. Other techniques that require measurements of all cracks that intersect a line (scanlines) tend to under-sample small cracks (La Pointe, 2002), making the scanline approach particularly inappropriate for geomorphology and weathering applications. For areas with large outcrop exposures, circular scanlines combined with a window approach have proven effective (Watkins et al., 2015). Here, we outline a 'window' approach that can be employed regardless of outcrop size or fracture density. We also detail an expansion of crack length



measurements – similar to that proposed by Weiss (2008) – so that long fractures are not underrepresented (see length methods below).

Importantly, the number and size of windows observed on each outcrop or at each site will depend on the typical number and size of cracks present on the surface of the rock (see section 4.2). It is preferable to strike a balance between window size and number so that during data analysis, variance can be quantified by comparing data collected between windows on the same outcrops and at the same site.

Choosing the placement of windows on the outcrop should entail a stratified random sampling approach. In other words, factors like aspect should be taken into consideration and controlled for as much as possible in the window placement strategy by, for example, only using upward facing surfaces. Then, window placement determination is made to avoid sampling bias and edge effects. For example, if upward facing outcrop surfaces are to be characterized, then the total length and width of the face could be employed to align sufficient numbers of windows along even intervals of those measurements (e.g., for example, three windows whose centers are located along the center axis of the rock, with even spacing between the edges and each box; Fig. 1b).

For the placement of each window, we recommend employing a simple cardboard template of the appropriate window size with a center hole and trace the outline with chalk directly on the clast or outcrop. Then, all crack measurements are made in the window(s). Each window should be numbered and photographed in the context of each outcrop or clast. Detailed photo-documentation and coordinates to 0.00000 dd are also recommended.

3.5 How many observation areas?

The number of clasts, outcrops, or windows required to measure sufficient cracks will vary with the study goals, site complexity, and the variables for which the data are being tested or controlled. Importantly, for each study, the required number of observation areas must be established based on the amount that is necessary to gain a statistically sufficient number of crack observations to represent the rocks in question for that setting (see section 4.2). As yet, no rule-of-thumb can be employed, because there has not been sufficient standard fracture data collected to establish such a rule – an illustration of the motivation of this paper! Rocks or outcrops with lower crack density (number of cracks per area) will require that larger areas of their surface be examined in order to measure sufficient cracks for statistical significance (see section 4.2). Thus, as an example only, we note that in past work, when State Factors were carefully controlled for, relationships between rock material properties and rock cracking properties were evident from about three to ten 10⁰-meter scale outcrops per rock type on ridge-forming quartz rich rocks (Eppes et al., 2018). However, we emphasize that until sufficient magnitude of datasets has been collected, the amount of observation area must be established based on the number of fractures available uniquely at each study site.

4 Standardized method: Selecting fractures for measurement

4.1 Rules-based criteria for selecting fractures in surface processes research

The term ‘fracture’ is employed with a wide variety of meaning across the geosciences, potentially resulting in large variations in the range of features that two individuals might study on a single outcrop (Long et al., 2019). Therefore, it is crucial to employ clear and repeatable rules-based criteria (e.g., Table 1) for what constitute measurable ‘cracks’ within any fracture-related research. To not do so consistently results in a high variance of subjective bias that is more reflective of worker personality than of the



variance in fracture of the outcrop (Andrews et al., 2019). Thus, consistency and documentation are required for deriving interpretable and repeatable results.

Our proposed rules (Table 1) for determining which fractures to measure at any given field site were developed in the context of surface processes research and through iterations with numerous non-expert users (undergraduate students) to arrive at criteria that provide consistency in observations across users. Because surface processes are frequently and largely dependent both on rock erodibility and water within a rock body, we limit our recommended criteria to apply only to open voids, which are known to greatly impact both. Also, because other types of open voids like vesicles are common in rock, we employ the additional criteria that the open void must be planar in shape, bounded by parallel or sub-parallel sides (hereafter fracture or crack ‘walls’), with a visible opening that is deeper than it is wide. Fracture walls will pinch together at fracture terminations.

It is common for such planar voids in rock to have been filled with mineral solids during intrusion and metamorphism, diagenesis, or weathering. Portions of fractures containing such cements do not meet the ‘open’ criteria and, thus, should not be included in the fracture dataset. However, voids that fit the shape criteria that are filled with lichens, dust, or other permeable material that can be readily brushed out with a fingernail or prodded with a needle should be included. If solid mineral cement forms a discontinuous bridge between fracture walls fully connecting the two walls of the otherwise open, planar void, the open length of the fractures on either side of the bridge would be treated as individual fractures. To distinguish this type of fracture truncation, a yes/no indication may be added to the dataset collected.

Finally, we also propose the criteria that the planar void must be continuously open (no ‘bridges’ of cemented mineral material) for a distance longer than 10 X the characteristic grain size dimension or 2 cm, whichever is greater. In most rock types, this translates to a 2 cm minimum cutoff for countable cracks (Fig. 2a; See section 5.4.1 below for measuring lengths). We propose this length threshold based on three features. First, past work has demonstrated that deriving precise (repeatable) detailed information -- other than length -- for cracks <2 cm in length is challenging (e.g., Eppes et al., 2010). Second, temperature-dependent acoustic emission measurements (Wang, et. al, 1989; Griffiths et al., 2017) and theoretical arguments suggest that on single year time scales, cracks on single grain and smaller length scales exist in thermodynamic equilibrium, (randomly) opening and closing under constant redistribution of ubiquitous diurnal to seasonal thermal stresses within surface rocks. The approximate statistical mechanical ‘rule-of-ten’ states that well-defined equilibrium and nonequilibrium, continuum-scale properties, e.g., viscosity, density, stress and strain, each determined by myriad microscale random processes, are obtained on length scales approximately 10 times an appropriate molecular length scale, e.g., average atomic size or mean free path length between colliding (gas) molecules. This interpretation is consistent with recommendations for the number of grains the minimum diameter of a sample is for repeatable testing of continuous rock properties such as rock strength and elastic moduli (ASTM, 2008 and 2017).

Last, and practically, the high abundance of cracks below this cutoff significantly increases the time required for crack measurement. If these smaller cracks are of interest, they can be characterized with photographic analysis (not covered herein), or subjected to semi-quantification via an index (see section 5.2). Importantly, in some applications it may be appropriate that a larger minimum threshold in crack length is chosen. However, in that case, crack abundances in the rock will possibly dictate that significantly larger observation areas of the rock exposure need to be employed in order to obtain sufficient numbers of cracks to provide representative data (see section 4.2).



Regardless of the threshold length chosen for the study, two adjacent fractures separated by intact rock or bridges of cement are considered two fractures, even if at a distance they appear to be continuous (Fig. 2b). This practice results in repeatable measurement between multiple workers and provides the most accurate representation of past crack growth and crack connectivity in the rock body.

4.2 Determining how many fractures to measure

Most published fracture-focused studies provide no justification for the number of fractures they measure, begging the question - is the dataset representative of the rock body? However, it is a long-recognized concept in fracture and rock mechanics that crack size distributions are highly skewed and characterized by scale-independent power law distributions (e.g. Davy et al., 2010; Hooker et al., 2014). Thus, the expected power-law distribution of fracture size can be leveraged in most cases to ensure that a representative crack population has been measured in any given dataset (Ortega et al., 2006).

Here, we recommend that to fully characterize the fractures for any site(s), outcrop(s), or feature(s) of interest, sufficient numbers of cracks should be measured such that a statistically robust power-law distribution in crack length is evident in the data. While other log normal, exponential, and Weibull distributions have been proposed for various fracture datasets (e.g., Baecher, 1983), employing these distributions depends on preexisting knowledge of the expected dataset. Thus, unless there is prior documentation of fracture distributions at a particular site, the power law distribution should suffice.

In practice, it is an iterative process to determine the number of fractures required for any given dataset, but generally, on the order of 10^2 cracks are required (e.g., Zeeb et al., 2013) to reach a representative distribution (Fig. 3). When sufficient numbers of cracks have been measured to result in such a distribution, then it can be assumed that the population of measured cracks is representative of all cracks on the rock, outcrop, or group of rocks/outcrops with certain features. For example, if the goal of a study is to test the influence of rock type on crack width, enough cracks must be measured to allow for a power-law distribution of crack lengths for *each* of the rock types. That population of cracks can then be considered representative of the given rock type, and statistics on other crack properties like width can also be reasonably interpreted as representative.

We provide an example of what that iterative process might look like in Fig. 3. In this example, all cracks were measured on the surface of 15-50 cm diameter granitic boulders selected along transects across both a modern wash bar (with few overall cracks per boulder) and a ~6 Ka alluvial fan bar (with many cracks per boulder). For the modern wash, after 5, 30, or 50 boulders, a statistically significant power law distribution is not evident (Fig. 3). However, after 130 clasts, the fit of the power law falls below a p-value threshold of 0.01. Thus, measurements from around 130 clasts were necessary to fully characterize cracks for that particular site. In contrast, the threshold p-value is reached after only 5 boulders for clasts with high crack density on the mid-Holocene age site; however, with more clasts examined, more variables per clast can be analyzed in the data. Thus, in order to evaluate different variables (like clast size or shape), the iterative process would repeat, but limiting the analysis to cracks found on clasts meeting the criteria of interest. In this example, a total of 130 clasts per surface were measured, enabling several subsets of data to be examined in order to test the influence on a range of clast properties on cracking.

One notable exception to the scale independent power law rule of thumb may be if there are abundant fracture terminations in infilling material. In this case, the size of the fracture (as defined by Table 1) is dictated by the spacing of the filled material bridges. Thus, fracture sets in rocks that contain abundant varnish or secondary precipitates like calcium carbonate may not follow this rule.



433 5 Proposed standardized baseline field data for fracture-focused surface processes research

434 Here, we describe the minimum suite of data (Table 2) that should be collected for all observation areas and all cracks. Table 3
 435 contains a list of recommended field equipment to make the measurements. The list of baseline data in Table 2 was developed with
 436 the goal of allowing the worker to fully analyze their fracture data in the context of variables known from the literature to influence
 437 or reflect cracking in exposed rocks. As overall knowledge of fractures in surface environments grows, the suggested set of
 438 measured variables should also change, just as, for example, the components of the simple stream power equation has evolved in
 439 fluvial geomorphology literature. The proposed fracture field methods list is also focused on direct ‘observables’ – without
 440 interpretation – that should apply universally across field areas. We readily acknowledge that additional items can and should be
 441 added to accommodate the needs of any specific study.

442
 443 The metrics listed in Table 2 and the associated methods described below are designed to be applicable and translatable to both
 444 natural outcrops and individual clasts. While they may also be applicable to fractures found in quarries and road-cuts, such outcrops
 445 are prone to cracking that has been anthropogenically induced by blasting, exhumation, and new environmental exposure (e.g.,
 446 Ramulu et al., 2009; He et al., 2012).

447 5.1 The ‘Crack Sheet’

448 We provide a data collection template comprising all the proposed standard data that allows efficient, complete, and detailed
 449 recording of all parameters while in the field (e.g., a “crack sheet”, Fig. 4 with digital version provided in supplemental data). The
 450 crack sheet can and should be modified to include additional parameters relative to any study. Ours is structured so that each
 451 observation area’s information (e.g., that of each clast, outcrop, or window) shares a row with the first crack measured. Then,
 452 subsequent rows are employed for additional measured cracks on the same observation area. Each observation area and crack are
 453 assigned unique identifiers to enable unambiguous reference in subsequent data analysis. Employing a ‘window’ rather than an
 454 entire clast or outcrop as the observation area necessitates slightly different data collection, so we provide two separate crack sheets
 455 in the supplement.

456
 457 The crack sheet provides a header space for site meta-data. Any observations that could elucidate the possible contributions of any
 458 State Factor (cl,o,r,p,t,T) acting at the site should be recorded (e.g., the vegetation or topography of the site). This header area
 459 should also be employed to note any and all criteria or conventions used throughout the study. For example, the use of any
 460 convention, such as right-hand rule for strike and dip measurements, should be noted in the header. The criteria employed to select
 461 clasts or outcrops (e.g., their size, composition, etc.) and the nature of the observation areas (ex: only the north face of all clasts;
 462 or entire exposed clast surface for all outcrops) should also be noted.

463 5.2 The use of semi-quantitative indices

464 We recommend employing indices for many observations following similar existing semi-quantitative methods commonly
 465 employed in both soil sciences (e.g., Soil Survey Staff, 1999) and sedimentology (e.g., rounding and sorting). The use of indices,
 466 rather than precise measurements, is especially appropriate for fractures and fracture characteristics, given the natural variation
 467 between different rocks, and the daunting number of measurements that would be required to accurately quantify, for example,
 468 something like total number of very small cracks.

469



Here, we define two particularly useful generic ‘abundance’ indices that are similar to those employed for quantifying the abundance of roots and pores in soils (Schoeneberger et al., 2012), whereby the quantity or coverage of specific elements or features is estimated within a specified area. For both, a ‘frame’ is employed whose size is dependent on the size of the feature being observed (Fig. 5). Features that are ≤ 0.5 cm are observed in 1 cm² frames; features >0.5 to <2 cm are observed in a 10 cm² frame; and features ≥ 2 cm are observed in a m² frame. Cut-out cardboard stencils of these sizes may be constructed and employed. The observer imagines randomly placing the ‘frame’ several times on any given portion of the observation area, noting the abundance of the feature of interest within the frame. The indices are based on the average value of abundance observed in any given such ‘frame’ across the entire area of observation (e.g., the entire clast, the entire outcrop, or the outcrop window).

The first index scales from 0 to 4 and is applicable for ‘countable’ features of interest in the research like small cracks, fossils, or large phenocrysts. The index is: none – 0 (no visible features in ANY frame), few – 1 (<1 feature on average), common – 2 (≥ 1 and <5 features on average), very common – 3 (≥ 5 and <10 features on average), and many – 4 (≥ 10 features on average).

The second index scales from 0 to 5 and is employed for features that are not readily counted nor consistent in size (like lichen, varnish, fine grained mafic, or felsic minerals). In these cases, the index is based on the percentage of the rock surface covered by the feature: none – 0; very little – 1 ($<10\%$); little – 2 (≥ 10 and $<30\%$); common – 3 (≥ 30 and $<60\%$); very common – 4 (≥ 60 and $<90\%$); and dominant – 5 ($\geq 90\%$). A percentage estimator (Fig. 6) should always be employed to assign the index categories – even experienced field workers are subject to ‘quantity bias’.

5.3 Measuring rock characteristics

The following rock characteristics should be measured for each observation area – each clast, outcrop, and/or window – that is employed in a study. Some cracking characteristics not captured in individual crack measurements are also included.

5.3.1 Clast, outcrop, or window dimensions

Rock – or outcrop – size, aspect, and slope can impact stress-loading through, for example, thermal stress distribution (e.g. Molaro et al., 2017; Shi, 2011). Or, for example, outcrop height has been linked to its exposure age and/or erosion rates (e.g., Hancock and Kirwan, 2007). The dimensions of the clast, outcrop, or window employed for fracture observations are also required for calculations of fracture density and intensity (i.e., the number/length of crack per unit area; see section 6.1).

The length and width of planar ‘windows’ are measured directly. If a window ‘bends’ across multiple faces of the rock surface, then separate length and width measurements should be made for each face with a distinct aspect. These areas are then added together for crack density and intensity calculations. The vast majority of rock clasts and outcrops found in nature have ‘prismatic’ forms (Domokos et al., 2020). Thus, length, width, and height of individual clasts or outcrops may be reasonably employed to calculate the exposed surface area (see section 6.1 for calculations).

For all dimension measurements regardless of rock shape, metrics are measured as point-to-point orthogonal measurements. Length is measured parallel to the longest axis. Width is measured on the widest extent that is perpendicular to length, and height is measured vertically from the uppermost surface of the rock down to the ground surface. If a through-going crack splits the rock into two pieces that remain *in situ*, it should still be considered one rock and measured accordingly. If a clast or outcrop is spheroidal in shape, that should be noted for future surface area calculations.



508

509 For site preservation, and to minimize geoheritage and environmental impacts, rocks should not be moved from their natural state;
 510 therefore, the height measurement of a highly embedded rock will only represent the height of the exposed rock surface above the
 511 ground. We have derived a metric to estimate the degree to which clasts are exposed vs. embedded (see section 5.3.8).

512 5.3.2 Sphericity and roundness

513 Sphericity and roundness from standard sedimentology practices (e.g., Krumbein and Sloss, 1951) provide metrics for rock shape.
 514 Shape can influence stress distribution in a mass and, therefore, cracking. For example, in general, corners tend to concentrate
 515 stresses, and ‘corner cracks’ are a recognized phenomenon in fracture mechanics (e.g., Kobayashi and Enetanya, 1976). Thus, we
 516 include this metric as one to be measured both for outcrops and for clasts.

517

518 Sphericity refers to the length by width ratio, or elongation, of the clast or outcrop, whereas roundness is a measure of angularity
 519 (Fig. 7). The roundness and sphericity designation for the square on the chart in Fig. 7 most closely matching the dominant shape
 520 of the entire clast or outcrop should be noted (ex. r-SR; s-SE). If a more precise rock shape analysis is needed, a modified Kirkbride
 521 device can be used to quantitatively measure rock roundness (see Cox et al., 2018 for device modifications and methodology).

522 5.3.3 Grain Size

523 Mean grain size can impact numerous fracture and stress characteristics including the proclivity for granular disintegration
 524 (Gomez-Heras et al., 2006), fracture toughness (Zhang et al., 2018), initial crack length, thermal stress disequilibrium (Janio De
 525 Castro Lima and Paraguassú, 2004), and bulk elastic properties (Vázquez et al., 2015). The mean grain size should be visually
 526 estimated by comparing the size of the dominant size of individual grains or mineral crystals to a standard grain size card. This
 527 size can be reported as one average value for all minerals, or different values for different suites of minerals (e.g., felsic vs. mafic),
 528 depending on the lithological assemblage(s) of the observation area(s).

529 5.3.4 Fabric

530 We employ the term ‘fabric’ to refer to any preexisting (prior to weathering) primary or diagenetic planar, linear, or randomly
 531 oriented anisotropies within the rock comprising the outcrop or clast of interest. Fabric is most commonly observed as fossils,
 532 lithological bedding planes, and/or diagenetic veins in sedimentary rocks, and as crystal horizons, foliation structures, and dikes in
 533 igneous or metamorphic rocks. Rock fabric can impart anisotropy that could influence cracking rates and orientations (e.g., Nara
 534 and Kaneko, 2006; Zhou et al., 2022). Any visible fabric type, as well as the strike(s) and dip(s) (or trend(s) and plunge(s)) of each
 535 parallel or subparallel set should be noted in the crack sheet for each observation area.

536 5.3.5 Cracks <2 cm in length

537 Cracks <2 cm in length can comprise a significant portion of all cracks on a given rock exposure, particularly in coarse crystalline
 538 rock types (e.g., Alneasan and Behnia, 2021). Thus, we recommend recording an index, using an observation ‘frame’ (see section
 539 5.2), that quantifies the abundance of cracks less than 2 cm in length (hereafter ‘small cracks’).

540

541 Observe the approximate number of small cracks visible each time the ‘frame’ is moved. Take a rough average of all theoretical
 542 frames and use the categories in Fig. 5 to assign an abundance. For example, if generally there are either zero or one small crack
 543 in any given 10 x 10 cm frame, the abundance would be “1” – i.e., few, <1 per unit area.



544 5.3.6 Granular disintegration

545 Granular disintegration refers to evidence of *active* loss of individual crystals or grains due to cracking along grain boundaries (i.e.,
 546 sedimentary particles or igneous or metamorphic crystals). This feature is observed on the rock surface as individual grains or
 547 small clusters of grains of the rock that can be brushed away with your hand. Granular disintegration is commonly observed in
 548 coarse igneous, metamorphic, and sedimentary rocks, and over the long-term leads to the accumulation of grus – sediment
 549 comprised of individual crystals – on the ground surface (Eppes and Griffing, 2010; Isherwood and Street, 1976; Gomez-Heras et
 550 al., 2006).

551
 552 This disintegration comprises the complete separation of intergranular cracking. Because the cracks that comprise granular
 553 disintegration are typically too small to be readily measured in the field, however, its presence is assumed when loose grains are
 554 present on the rock surface. The worker should mark yes (circle the ‘G’ on the Crack Sheet) if there is evidence of granular
 555 disintegration on the rock surface of observation. If more detail is desired, an abundance index (e.g., Fig. 5) may be employed to
 556 quantify what percentage of the surface of observation contains loose grains.

557 5.3.7 Pitting

558 Pitting is the occurrence of small holes or fissures that form on the rock surface due to granular disintegration or to preferential
 559 chemical weathering of certain mineral types, typically feldspars and micas in silicate rocks. Pitting is distinct from granular
 560 disintegration as it is not necessarily ‘actively’ occurring – i.e., pitting can exist without loose grains on the rock surface. We
 561 include it as a rock property related to fracture because of its possible linkage to intergranular cracking. Furthermore, measuring
 562 the extent and depth of pitting due to chemical weathering has long been employed as a relative age dating tool in Quaternary
 563 geology applications (Burke and Birkeland, 1979).

564
 565 Pitted surfaces form as individual grains become weathered and fall out or are dissolved; or, for soluble rocks like carbonates, as
 566 entire rock regions are dissolved. Pitting can either be quantified as present/absent (circle P on the crack sheet) or as a quantity
 567 index (Figs. 4 and 5).

568 5.3.8 Clast exposure

569 This metric is used to record to what degree individual clasts appear to be exposed above the ground surface. Individual clasts are
 570 known to weather and erode from the upper rock surface down until they become ‘flat’ rocks at the ground surface (e.g., Ollier,
 571 1984). Surface exposure can be estimated as the amount and shape of a boulder’s exposed surface that is currently not covered by
 572 loose sediment, vegetation, or other material. We grouped this exposure into four categories: 0 -- the clast is sitting above the
 573 ground, and its sides curve downward toward the ground surface almost meeting; 1 -- the clast is partially covered, with sides
 574 curving downward toward the ground surface but not meeting; 2 -- the clast is “half” covered, with sides projecting roughly
 575 vertically into the ground surface; 3 -- the clast has only one upward facing side visible at the ground surface. In a field study, a
 576 correlation test on data from 300 boulders revealed a positive correlation of 0.66 between the indices and the fraction of boulder
 577 embeddedness (in vertical length) (Shaanan et al., 2022).

578 5.3.9 Lichen and varnish

579 Lichens and other plant life can act to push rocks apart during growth (Scarciglia et al., 2012), but have also been shown to
 580 strengthen rocks through infilling of voids or shielding from stress-inducing sunlight (Coombes et al., 2018). We note that lichen



are living organisms that would be killed by removal. In order to determine if a lichen-coated lineation is in fact a measurable fracture (see section 4.1), a needle or straight pin may be employed to poke through the lichen into the possible void of the crack.

Rock varnish (oxide staining that can appear as a dark gray/black or orange coating on rock and typically contains Fe or Mn oxides) is well-documented to evolve over time. The extent of varnish cover has been employed frequently as a relative-age indicator, particularly in arid environments (e.g., McFadden et al., 1985; Macholdt et al., 2018). Thus, variations in varnish across the rock face can provide evidence of loss of surface material through *in situ* cracking.

Lichen and varnish can come in many forms and be difficult to distinguish from each other and from primary rock minerals, hiding in cracks, pitting holes, and atop mafic crystals. So, careful consideration of the types of lichen and varnish that may be found in field site and close inspection with a hand lens is recommended. A fresher exposure of the rock surface can help in the identification of lichen and varnish relative to the natural rock composition and color. Due to the geodiversity impact, however, do not make such exposures with force.

The quantity of lichen and varnish (secondary chemical precipitates deposited on the subaerial rock surface) visible on the rock observation surface are separately estimated using a visual percentage estimator (Fig. 6) and a quantity index is assigned (Fig. 5; Section 5.2).

5.4 Crack characteristics

The following properties are measured for each crack found within the observation area that meets all the crack selection criteria listed in Table 1.

5.4.1 Length

Crack length is measured for the entire surface exposure length of the crack; i.e., around corners and up and down rock topography (Fig. 2a). Measurements can be made with flexible seamstress tape to follow the curve of a crack's exposure on the rock surface. Length is only measured where there is an open void (Fig. 2b; Section 4.1). If a seemingly continuous crack (Fig. 2b, left) is in fact separated by bridges of solid rock (Fig. 2b, right inset), then these should be measured as two different cracks and their lengths should terminate at the rock bridges. The inset in Fig. 2b reveals four cracks possibly meeting all Table 1 criteria. Photographs do not allow the 3D visualization required to determine if there is open void along the entire length. The precise length of the smaller cracks would be needed to determine if they meet the 2 cm/10 grain cutoff.

Importantly, when using a 'window' approach to rock observation area, both the total length of the crack extending beyond the window, as well as the total length within the window, should both be recorded. The latter is employed in crack intensity calculations (section 6.1); the former provides representative information about all crack lengths on the rock being measured.

5.4.2 Width

Crack aperture widths (hereafter, 'widths') can impact both the strength and permeability of rock. Generally, they scale with crack length and thus can possibly reflect the innate subcritical cracking parameters of the rock (Olson, 2004). Crack widths typically vary along their exposure and pinch out at crack tips. Determining an average or representative width can thus be somewhat arbitrary and subject to bias. Locating the widest aperture is less subject to bias and can also provide information about cracking



processes. Thus, we recommend consistently recording crack width at the midpoint of the measured length of the exposed crack and also recording its maximum width along its exposure.

Both measurements should only be made in regions of the crack where crack walls are parallel or sub-parallel (e.g., green arrows in Fig. 8), avoiding locations where crack edges have been obviously rounded by erosion or chemical weathering, or where large pieces have been chipped off or are missing (e.g., red arrows in Fig. 8). If it is unclear if a portion of the crack has chipped off (e.g., orange arrow in Fig. 8), a notation can be made and employed later to eliminate potential outliers in the dataset. Cracks greater than about 3 mm in width can be easily measured by inserting the back-blades of digital calipers into the widest opening of the crack. For narrower cracks, a ‘crack comparator’ (Fig. 7) is recommended, whereby the line on the comparator most closely matching the crack aperture is chosen.

5.4.3 Strike and dip

Crack orientation (i.e., strike and dip) is a function of the orientation of existing anisotropy within the rock and the orientation of the principle stresses that drove its propagation. There is a common misperception that preferred crack orientations are solely related to tectonic forces; however, both gravitational and environmental stresses can also be directional (e.g., St. Clair et al., 2015; McFadden et al., 2005). When cracks are growing at subcritical rates, they can lengthen through a series of ‘jumps’ that link parallel or subparallel smaller fractures. The following suggestions are for research aimed not at characterizing these small heterogeneities, but rather identifying major stresses and heterogeneity in the entire rock body.

Crack orientation is measured with a geological compass or similar tool that has both azimuthal direction and inclinometer functionality. When measuring strike and dip of cracks, it is important to visualize how the crack plane intersects the rock surface, as if you were to slip a sheet of paper into the ‘file folder’ of the fracture. For larger cracks, there may be different dips on either side of the crack due to weathering of the crack opening, so it is imperative to measure the angle at the interior of the crack where its walls are parallel (Fig. 8).

Cracks grow until they intersect other cracks. If cracks appear to intersect or branch (i.e., two connected planar voids with noticeably different orientations), their total length should be measured as one crack, but their orientations should be measured separately (e.g., two strikes and dips for the single crack). For cracks that meander around small heterogeneities like phenocrysts or fossils, the overall trend is measured. For curvilinear cracks, the average orientation can be measured, as the orientation of the non-curved plane whose ends are defined by the ends of the crack. Alternatively, the crack curvilinear plane may be subdivided into roughly linear planes and each orientation measured. It is important to note which method was employed and to remain consistent for all measurements.

There are numerous commonly-employed conventions for measurements of strike and dip. If the worker is consistent and clear in their use of their preferred convention and in the presentation of their data, any are acceptable. If the worker has no such prior habits, we recommend recording strikes as an azimuthal orientation from 0-359 degrees, and dip angle as an angle deviation from horizontal of 0-90 degrees. For dip direction, we also recommend employing a convention such as the “right-hand rule,” whereby the dip direction is always known from the orientation of the strike alone. For example, the right-hand rule states that the down-dip direction is always to the “right” of the measured and recorded strike when the observer is facing the same direction of the



656 strike. Therefore, the strike that is recorded is the one whereby the dip direction is always +90 degrees clockwise (to the right)
 657 from the strike direction.

658 5.4.4 Fracture parallelism

659 Noting the parallelism of the cracks can help to better understand the origins of the population of fractures at a site. Parallelism is
 660 common because cracks often follow rock heterogeneities or anisotropies such as bedding, foliation, veins, or even the rock surface.
 661 Fractures in a single bedrock outcrop or clast are also commonly parallel because they have formed due to external stress-loading
 662 with a consistent orientation (e.g., those related to tectonics or directional insolation). Thus, noting parallelism may help to
 663 distinguish the origins of fractures, though not always. For example, ‘surface parallel cracks’ (e.g., Fig. 2a) - commonly referred
 664 to as exfoliation, sheeting joints (e.g., Martel, 2017), or spalling – vary dramatically in scale and can have origins related to several
 665 different factors including tectonic-topographic interactions (Martel, 2006), chemical weathering and volumetric expansion (Røyne
 666 et al., 2008), and thermal stresses related to insolation (e.g. Lamp et al., 2017; Collins and Stock, 2016) and fire (e.g. Buckman et
 667 al., 2021).

668
 669 In the crack sheet, note to which features the crack is parallel. A visual inspection will suffice for most applications, but for
 670 occasions where more precision is needed, the crack may be considered parallel if the strike and dip of a crack is within $\pm 10^\circ$ of
 671 the orientation of the feature (the rock’s long axis, its fabric, or its outer surface). A crack may be parallel to more than one feature
 672 in the rock. Add categories as necessary for rocks with other repeating features unique to the field site (fossils; veins, etc.).

673 5.4.5 Sheet height

674 Surface parallel fractures naturally detach ‘sheets’ of rock between the fracture and the rock surface (‘h’ in Fig. 2a). The thickness
 675 of these sheets may be of interest for understanding the size of sediment produced from the fracture or for understanding the
 676 stresses that produced the fracture. Sheet height is measured using calipers at the location of the maximum height of the sheet and
 677 is only used for surface parallel cracks. To limit these measurements to those that have likely formed in situ as related to the current
 678 morphology of the rock, a rule of thumb is to only measure those ‘sheets’ that would result in removal of $<10\%$ from the outer
 679 surface of the rock downward into the dimension(s) of the rock face(s) to which they are perpendicular.

680 5.4.6 Weathering index

681 Rock fracture is ultimately a molecular scale bond-breaking process; so, when cracks propagate, they initially form a razor-sharp
 682 lip or edge. Over time, these edges naturally round through subsequent chemical and physical weathering, erosion, and abrasion
 683 (e.g., regions of the red arrows in Fig. 8).

684
 685 We have established an index of relative degree of such rounding along a crack edge to be noted in the crack sheet:

- 686
- 687 1: fresh with evidence of recent rupture (flakes/pieces still present, but not attached)
- 688 2: sharp, no rounded edges anywhere
- 689 3: mostly sharp with occasional rounded edges
- 690 4: mostly rounded edges with occasional sharp edges
- 691 5: all rounded edges
- 692
- 693



694 6 Suggestions for Data analyses

695 For initial data exploration, normal cross-plots or quantile-quantile plots (as well as standard correlation analysis) may be applied
 696 to rock and crack data. For categorical data, normal analytical techniques (histograms, discrete correlation analysis, etc.) can be
 697 applied. As with all heavy-tailed data, the median is preferred over the mean value to understand a characteristic value—though
 698 power distributed data generally does not have a characteristic dimension. Standard statistics such as mean, variance, skewness,
 699 and kurtosis all remain valid to explore and evaluate the datasets.

700 To understand crack length and crack width data, it is key to first recognize that, with the exception of studies such as in rocks
 701 with cracks with uniform spacing and bedding-controlled widths (Ortega et al., 2006), the data will have a heavy-tailed distribution,
 702 such as lognormal, gamma, or power law. As we mention above, of these, strong observational and theoretical evidence suggests
 703 that fracture size is most commonly power law distributed (Bonnet et al., 2001; Davy et al., 2010; Hooker et al., 2014; Ortega et
 704 al., 2006; and Zeeb et al., 2013), i.e.,

$$705 \quad n(b) = Ab^{-\alpha} \quad (1)$$

706 where b is the crack dimension (length or width) of interest, n is the number of cracks with dimension d , and A and α are constants.
 707 When log-transformed, Eq. (1) becomes

$$708 \quad \log(n(b)) = \log(A) - \alpha \log(b) \quad (2)$$

709 which has led many practitioners to fit Eq. (2) by linearly binning the data in n , then log-transforming the data and fitting the
 710 resulting data with a linear regression. This has proven to lead to significant bias in estimates, $\hat{\alpha}$, of the power law exponent
 711 (Bonnet et al., 2001; Clauset et al., 2009; Hooker et al., 2014) and is not recommended despite its common usage.

712 Two straight-forward approaches have been shown not to have biases, or misestimates of the exponent α . 1) The following is based
 713 on Clauset et al., (2009). First, the exponent can be found from the cumulative distribution of the dimensions, $C(b)$, or number of
 714 fractures with dimension greater than b , i.e.,

$$715 \quad C(b) = \int_b^{b_{\max}} n(b) db \quad (3)$$

716 Where b_{\max} is the maximum size of the crack dimension (e.g., maximum length or width). The cumulative power law distribution
 717 has the form

$$718 \quad C(b) \propto b^{1-\alpha} \quad (4)$$

719 It is common to denote $1-\alpha$ as c . To find α (or c), the dimension data is logarithmically binned. In other words, the dimension data
 720 is binned on a logarithmic (1, 10, 100, ...) frequency scale, and then log-transformed. At this point, linear regression techniques
 721 can be applied to estimate α and assess uncertainty. However, in all cases, uncertainty estimates such as R^2 will overestimate the
 722 certainty for such log-transformed data; but at least the estimate of α is unbiased.

723 2) Another method to find α from a data set of crack dimensions is to use the maximum likelihood estimator (MLE) given by

$$724 \quad \hat{\alpha} = 1 + N \left[\sum_{i=1}^N \ln \left(\frac{b_i}{b_{\min}} \right) \right]^{-1} \quad (5)$$



where $\hat{\alpha}$ is the estimate of the exponent in (1), b_i is the dimension of the i th crack, b_{min} is the minimum valid crack dimension (see below) and N is the total number of samples (Clauset et al., 2009; Hooker et al., 2014). The MLE estimate has the advantage of an accurate estimate of standard error, σ , given by

$$\sigma = \frac{\hat{\alpha}-1}{N} + O\left(\frac{1}{N}\right). \quad (6)$$

Clauset et al., (2009) showed that both the logarithmically-binned cumulative distribution and the MLE estimator produce unbiased estimates of the exponent. For all empirical power law distributions, there is a scale, in our case b_{min} , below which power law behavior is not valid. This can be visually assessed by plotting Eq. 2 with logarithmically binned n . The interval between b_{min} and b_{max} where the slope is linear is where the power law is valid (Clauset et al., 2009; Ortega et al., 2006); Clauset et al. (2009) presents a formal method to find b_{min} and b_{max} . Hooker et al. (2014) use a χ^2 test to evaluate the goodness of fit, which is simpler than the p-tests of the Kolmogorov-Smirnov statistic proposed by Clauset et al. (2009).

735

736 6.1 Crack density and intensity

In fracture mechanics literature, crack density commonly refers to the number of cracks per unit area (e.g., # cracks/m²), and crack intensity refers to the sum length of all cracks per unit area (e.g., cm/m²). However, these terms are interchanged in some literature. It is therefore important to define them in each usage; and for clarity, the term ‘number density’ might be employed.

740

In either calculation, the ‘area’ refers to the surface area of observation area. For cracks measured in ‘windows’ (section 3.4), use the length of cracks only *within* the window and the area of the window (e.g., 10 cm x 10 cm) for the calculations. For loose clasts and outcrops, the appropriate calculation of surface area will depend on the shape and angularity of the rock. For most rocks, calculations for the surface area of the exposed sides of a rectangular cuboid ($L*W + 2*(L*H) + 2*(W*H)$) are appropriate.

745 6.2 Circular Data

Standard ‘linear’ statistics cannot be employed for circular data. We suggest the use of circular statistical and plotting software for the visualization and analysis of strike and dip data. The statistics employed by such software is typically based on established circular statistical research methods (e.g., Mardia and Jupp, 1972; Fisher, 1993). The following statistics are useful in reporting strike and dip data.

750

The Mean Resultant Direction (a.k.a. vector mean, mean vector) is analogous to the slope in a linear regression. Circular variance can be quantified using either a Rayleigh Uniformity Test (for single mode datasets) or a Rao Spacing Test (for datasets with multiple modes), whereby p-values <0.05 indicate non-random orientations. If p-values for these tests are below a threshold (e.g., <0.05), then data are considered non-uniform or non-random.

755

The Rayleigh statistic is based on a von Mises distribution (i.e., a normal distribution for circular data) of data about a single mean (i.e., unimodal data). Therefore, for multi-modal data, the variance might be high, but nevertheless, the data might be non-uniform.

The Rayleigh Uniformity Test calculates the probability of the null hypothesis that the data are distributed in a uniform manner. Again, this test is based on statistical parameters that assume that the data are clustered about a single mean.

760



Rao's Spacing Test is also a test for the null hypothesis that the data are uniformly distributed; however, the Rao statistic examines the spacing between adjacent points to see if they are roughly equal (random with a spacing of $360/n$) around the circle. Thus, Rao's Spacing Test is appropriate for multi-modal data and may find statistical significance where other tests do not.

8 Case Example

To demonstrate the consistency of results that might be achieved across users, we provided minimal training (one demonstration with some minor oversight of initial work) to four groups of two students each. The fifth pair of workers included a scientist who had logged over 500+ hours of experience using the standardized methods. Each of the five groups followed the methods to measure the length and abundance of cracks on boulders (15-50 cm max diameter) on the same geomorphic surface (a 6000-year-old alluvial fan in Owens Valley California, comprised of primarily granitic rock types). Each group followed the methods described herein for rock and crack selection and measurements. As such, the results from each group (Fig. 9; Data Supplement) could be compared not only for crack selection and measurements, but also for observation area selection – a key component of collecting data that is representative of a particular site.

We find that the data collected by each of the groups for crack length, number of cracks per rock and rock size are statistically indistinguishable by student t-test (all pairs of p-values > 0.1 ; Fig. 9; Data Supplement). Also, there is no consistent difference between measurements made by the novice groups and that of the trained group. The mean crack lengths from the four novice groups (37±23 mm to 59±51 mm) span across that of the mean collected by the well-trained group (42±22 mm; Supplement), as do the number of cracks per rock (2 ± 2 to 6 ± 8 for novice groups compared to 3 ± 3 for trained group). With only one exception (crack length for group 1) variance between groups does not range by more than a factor of 3 in any of the data – a common rule of thumb for the threshold of 'similar' variance between small datasets. Overall, especially given the relatively small size of the datasets (~10-20 rocks and ~40-60 cracks each), this comparison suggests that the results using the standardized methods are reproducible, even with novice workers with minimal training.

9 Conclusions

The methods proposed herein comprise a standardization of field data collected in rock fracture research surrounding surface processes and weathering-based geologic problems. These methods comprise best practices extracted from existing research and methods that have been developed in the context of structural geology and fracture mechanics research, while also providing general guidance and nuances developed from experiences (and mistakes) over the last two decades of fracture-focused field research applied to geomorphology and soil science. It is our hope that providing these detailed, accessible, standardized procedures for gathering and reporting field-based crack data will open the door to rapidly building a rigorous galaxy of new datasets as these guidelines and methods become more widely adopted. In turn, they may enable future workers to better compare and merge fracture data across a wide range of studies, permitting future refinements of our understanding of rock fracture and in the methods themselves. Compiling such a standardized global dataset is the best hope for fully characterizing the role and nature of fractures in Earth surface systems and processes.

10 Author Contributions

MCE spearheaded evolution of the development of the guiding principles and methods described herein as well as writing of the manuscript. JA, SB, MD, SE, FM, SP, MR, and US all participated extensively in field campaigns during which the methods were developed and refined, and they contributed to editing of manuscript and editing and development of figures. MM, AR and RK



798 contributed to the development of theoretical statistical analyses practices that are outlined in the document and the editing of the
799 manuscript.

800 **11 Competing interests**

801 The authors declare that they have no conflict of interest.

802

803 **12 Data Availability**

804

805 All data presented in the manuscript are available in the Supplement.

806 **13 Acknowledgements**

807 The body of knowledge presented herein was derived in large part over the course of research funded by the National Science
808 Foundation Grant Nos. EAR#0844335 (with supplements #844401, #0705277), #1744864, and #1839148 and NASA ROSES
809 Mars Data Analysis Program award #NNX09AI43G. Several photographs in figures were cropped and employed with permission
810 from Marek Ranis, Artist-in-Residence for NSF #1744864. In addition, the authors wish to acknowledge the contributions from
811 countless undergraduate and graduate students who contributed to the application and development of these methods in classes
812 taught by MCE at the University of North Carolina at Charlotte.

813

814

815



Figure Captions

Fig. 1. Images illustrating the selection of observation areas for clasts and outcrops. A. Photograph of a transect established for clast selection. Black dot: predefined transect interval location on the tape. Red dot: clast that does not fit the predefined clast selection criteria (e.g., it is too big). Green dot with red circle: clast that fits criteria but is further away from the interval point than the clast with the green dot. Green dot: closest clast to the transect interval that meets the selection criteria. B. Annotated photograph showing an idealized placement of ‘windows’ (dashed black squares) on a bedrock outcrop. Outcrop dimensions are measured and the windows are placed using predetermined selection criteria. In this example, the windows are equally spaced along the centerline of the long-dimension of the upward-facing side of the outcrop.

Fig. 2. A. Example of the measurement of a surface exposure length (L ; yellow line) of a crack meeting the criteria in Table 1. The ‘h’ refers to the location where sheet height would be measured for this surface parallel crack. B. Example of fractures that may appear to be a single fracture (left), but upon close examination are in fact multiple fractures intersecting and/or separated by rock (right inset). Arrow points to the location of the inset image on the main image. Compass in the foreground for scale.

Fig. 3. Example histograms and statistics of crack length data measured on the exposed surfaces of clasts 15–50 cm max diameter. Upper row are data for clasts found on a modern ephemeral stream boulder bar. Clasts overall have very low crack density. Lower row are data for clasts on an ~6.2 ka surface where crack density is much higher. Note that it takes about 100 clasts to arrive at a statistically significant power law distribution for the Modern Wash clasts, but only 5 rocks for the rocks with higher crack densities. Producing histograms interactively as data is collected can help establish how many observation areas are necessary for a given site.

Fig. 4. Reduced size image of an 8.5” x 11” ‘crack sheet’ to be employed in the field to increase efficiency and to reduce ‘missing’ data. Sheet templates for both clasts and outcrops that can be modified are provided in Data Supplement as well as a data-entry template.

Fig. 5. Visual aide for estimating the abundance of “countable” rock features – including cracks. An index of 0–4 is assigned depending on the abundance of features within an average of any given observation area (ex: 10 x 10 cm) on the clast or window being examined. The area of observation is defined by the size of the features being measured. A 10 cm x 10 cm square is used for estimating the abundance of ‘cracks < 2 cm’ defined as cracks with lengths of ~0.5 cm but < 2 cm (see section 5.2 for details of how to use the index). For features ≤ 0.5 cm, a 1 cm x 1 cm area would be employed and for features ≥ 20 mm, a 1 x 1 m area.

Fig. 6. A visual percent estimator (modified from Terry and Chilingar, 1955). Estimator should be employed in every estimate of percentages. See section 5.2 for using the estimator to assign a percent coverage index to features that are not countable or vary in size (e.g., lichen coverage, fine mafic minerals, etc.).

Fig. 7. **Inset:** Roundness and sphericity chart – modified from Krumbein and Sloss (1951). **Roundness:** A = angular; SA = subangular; SR = subrounded; R = rounded; WR = well-rounded. **Sphericity:** S = spherical; SS = subspherical; SE = sub-elongate; E = elongate. **Edges:** crack comparator whereby the width most closely matching the crack aperture is noted. Note: a to-scale pdf is available in the Data Supplement, however, owing to printing and publication scaling, it is highly recommended to calibrate the comparator prior to using it in the field.

Fig. 8. Examples of aperture transects that are appropriate for measurement of crack aperture widths (green) and transects where there is evidence that the crack walls have been eroded or chipped and therefore should not be employed for a width measurement (red). In cases where it is not clear if erosion or chipping has occurred (orange), a note can be made for the crack width to possibly eliminate outliers during data analysis.

Fig. 9. Box and whisker plots of data case example data collected by five different pairs of workers on the same geomorphic surface. “x”s mark the means. Groups 1–4 were novice workers. Group 5 comprised one experienced worker. A. Crack lengths B. Cracks per rock C. Clast length



867

868 **Table 1. List of proposed rule-based criteria for defining measurable cracks**

The answer to the following questions must be 'yes' for all measured cracks. Measure <u>all cracks meeting these criteria</u> within the observation area.	<u>NOTES</u>
<ul style="list-style-type: none"> Is the feature a lineament longer than it is wide? Does the lineament contain open space bounded by walls? If the lineament is not open, can the infilling material (ex: dust and lichens) be readily scraped out? If the lineament is open or after the material has been scraped out, is the opening deeper than it is wide <u>and</u> bounded by ~parallel walls? Is the open portion of the lineament ≥ 2 cm (>10 grains) in length (without interrupting bridges of cemented infilling material)? 	Do not measure: <ul style="list-style-type: none"> Spherical pores/vesicles. Lineaments, or portions of lineaments, with solid mineral infilling/cement. Ledge edges or linear etchings.

869

870 **Table 2. List of proposed data to collect for the rock observation area and for all cracks ≥ 2 cm in length**

871

Rock Observations	Crack Observations
<ul style="list-style-type: none"> Dimensions of the observation area (e.g. clast, outcrop, and/or window length, width, height) Rock Type Grain Size Mineralogy % (minimally felsic vs. mafic) Sphericity of Exposure Roundness of Exposure Fabric Description: strike, dip, type (i.e. vein, foliation, bedding) Evidence of Granular Disintegration: define an index Evidence of Pitting: define an index Lichen or Varnish: % 	<ul style="list-style-type: none"> Length: surface exposure length measured with a flexible tape Aperture Width: center and maximum widths as measured with crack comparator or calipers Strike: right hand rule preferred Dip: 0-90 degrees Parallelism: Note features parallel to crack (fabric, rock faces) Weathering characteristics: an index of rounded edges where 1 = entirely sharp, fresh edges; 2=mostly sharp edges, some rounding; 3 = mostly rounded edges, some sharp; 4= entirely rounded edges Sheet Height: the thickness of what would be the detached spall or sheet of rock (only if crack is surface parallel and it were to detach the rock surface)

872

873

874 **Table 3. List of field equipment**

Required	Recommended
<ul style="list-style-type: none"> Hand lens (large, 10x) Grain size card Crack comparator (for crack widths) Flexible seamstress tape measure (with mm) Calipers (mm 0.0 to 150) Brunton or similar compass Roundness and sphericity chart Visual percentage estimator Crack sheets 	<ul style="list-style-type: none"> Camera with macro lens Chalk for marking measured cracks and windows Safety pin or needle for crack exploration Cardboard cutout frames for windows Small white board or chalk board for including observation area ID in photos

875

876



877 Bibliography

- 878 Aich, S. and Gross, M. R.: Geospatial analysis of the association between bedrock fractures and vegetation in an arid environment,
879 International Journal of Remote Sensing, 29, 6937-6955, 10.1080/01431160802220185, 2008.
- 880 Al-Fahmi, M. M., Hooker, J. N., Al-Mojel, A. S., and Cartwright, J. A.: New scaling of fractures in a giant carbonate platform
881 from outcrops and subsurface, Journal of Structural Geology, 140, 104142, <https://doi.org/10.1016/j.jsg.2020.104142>, 2020.
- 882 Aldred, J., Eppes, M. C., Aquino, K., Deal, R., Garbini, J., Swami, S., Tuttle, A., and Xanthos, G.: The influence of solar-induced
883 thermal stresses on the mechanical weathering of rocks in humid mid-latitudes, Earth Surface Processes and Landforms, 41, 603-
884 614, 2015.
- 885 Alneasan, M. and Behnia, M.: An experimental investigation on tensile fracturing of brittle rocks by considering the effect of grain
886 size and mineralogical composition, International Journal of Rock Mechanics and Mining Sciences, 137, 104570,
887 <https://doi.org/10.1016/j.ijrmms.2020.104570>, 2021.
- 888 Anderson, T. L.: Fracture Mechanics: Fundamentals and Applications, Third, Taylor & Francis Group, Boca Raton, FL, 2005.
- 889 Andrews, B.J., Roberts, J.J., Shipton, Z.K., Bigi, S., Tartarello, M.C. and Johnson, G., 2019: How do we see fractures? Quantifying
890 subjective bias in fracture data collection. Solid Earth, 10, 487-516, 2019.
- 891 ASTM, 2008, Standard test method for splitting tensile strength of intact rock core specimens, ASTM D 3967-08.
- 892 ASTM, 2017, Standard test methods for compressive strength and elastic moduli of intact rock core specimens under varying states
893 of stress and temperatures, ASTM D7012-14, doi: 10.1520/D7012-14Atkinson, B. K.: Fracture Mechanics of Rock, Academic
894 Press Geology Series, Academic Press Inc., Orlando, Florida, <https://doi.org/10.1016/C2009-0-21691-6>, 1987.
- 895 Atkinson, B. K., Ed.: Fracture Mechanics of Rock, Academic Press Limited, San Diego, California, 1987
- 896 Ayatollahi, M. R. and Akbardoost, J.: Size and Geometry Effects on Rock Fracture Toughness: Mode I Fracture, Rock Mechanics
897 and Rock Engineering, 47, 677-687, 10.1007/s00603-013-0430-7, 2014.
- 898 Baecher, G. B.: Statistical analysis of rock mass fracturing, Journal of the International Association for Mathematical Geology, 15,
899 329-348, 10.1007/BF01036074, 1983.
- 900 Borg, I., Handin, J.: Experimental deformation of crystalline rocks: Tectonophysics 3, 249-367, 1966.
- 901 Berberich, S.: A chronosequence of cracking in Mill Creek, California, Geography and Earth Sciences, The University of North
902 Carolina Charlotte, ProQuest, 2020.
- 903 Birkeland, P. W.: Soils and Geomorphology, Oxford University Press, New York, New York, 1999.
- 904 Bonnet, E., Bour, O., Odling, N.E., Davy, P., Main, I., Cowie, P. and Berkowitz, B.: Scaling of fracture systems in geological
905 media, Reviews of geophysics, 39(3), pp.347-383, 2001.
- 906 Brantley, S. L., Eissenstat, D. M., Marshall, J. A., Godsey, S. E., Balogh-Brunstad, Z., Karwan, D. L., Papuga, S. A., Roering, J.,
907 Dawson, T. E., Evaristo, J., Chadwick, O., McDonnell, J. J., and Weathers, K. C.: Reviews and syntheses: on the roles trees play
908 in building and plumbing the critical zone, Biogeosciences, 14, 5115-5142, 2017.
- 909 Brantut, N., Heap, M. J., Meredith, P. G., and Baud, P.: Time-dependent cracking and brittle creep in crustal rocks: A review,
910 Journal of Structural Geology, 52, 17-43, 2013.
- 911 Brilha, J., Gray, M., Pereira, D. I., and Pereira, P.: Geodiversity: An integrative review as a contribution to the sustainable
912 management of the whole of nature, Environmental Science & Policy, 86, 19-28, <https://doi.org/10.1016/j.envsci.2018.05.001>,
913 2018.
- 914 Buckman, S., Morris, R. H., and Bourman, R. P.: Fire-induced rock spalling as a mechanism of weathering responsible for flared
915 slope and inselberg development, Nature Communications, 12, 2150, 10.1038/s41467-021-22451-2, 2021.



- 916** Burghilea, C., Zaharescu, D. G., Dontsova, K., Maier, R., Huxman, T., and Chorover, J.: Mineral nutrient mobilization by plants
917 from rock: influence of rock type and arbuscular mycorrhiza, *Biogeochemistry*, 124, 187-203, 10.1007/s10533-015-0092-5, 2015.
- 918** Burke, R. M. and Birkeland, P. W.: Reevaluation of multiparameter relative dating techniques and their application to the glacial
919 sequence along the eastern escarpment of the Sierra Nevada, California, *Quaternary Research*, 11, 21-51, 10.1016/0033-
920 5894(79)90068-1, 1979.
- 921** Burnett, Benjamin N., Grant A. Meyer, and Leslie D. McFadden.: Aspect-related microclimatic influences on slope forms and
922 processes, northeastern Arizona. *Journal of Geophysical Research: Earth Surface*, 113, 2008.
- 923** Buss, H. L., Sak, P. B., Webb, S. M., and Brantley, S. L.: Weathering of the Rio Blanco quartz diorite, Luquillo Mountains, Puerto
924 Rico: Coupling oxidation, dissolution, and fracturing, *Geochimica et Cosmochimica Acta*, 72, 4488-4507, 2008.
- 925** Chilton, K. D. and Spotila, J. A.: Preservation of Valley and Ridge topography via delivery of resistant, ridge-sourced boulders to
926 hillslopes and channels, Southern Appalachian Mountains, U.S.A., *Geomorphology*, 365, 107263,
927 <https://doi.org/10.1016/j.geomorph.2020.107263>, 2020.
- 928** Clauset, A., Shalizi, C.R. and Newman, M.E.: Power-law distributions in empirical data. *SIAM review*, 51, 661-703, 2009.
- 929** Collins, B. D. and Stock, G. M.: Rockfall triggering by cyclic thermal stressing of exfoliation fractures, *Nature Geoscience*, 9, 395-
930 401, 2016.
- 931** Coombes, M. A., Viles, H. A., and Zhang, H.: Thermal blanketing by ivy (*Hedera helix* L.) can protect building stone from
932 damaging frosts, *Nature: Scientific Reports*, 8, 1-12, 2018.
- 933** Cox, R., Lopes, W. A., and Jahn, K. L.: Quantitative roundness analysis of coastal boulder deposits, *Marine Geology*, 396, 114-
934 141, <https://doi.org/10.1016/j.margeo.2017.03.003>, 2018.
- 935** Cuccuru, S., Casini, L., Oggiano, G., and Cherchi, G. P.: Can weathering improve the toughness of a fractured rock? A case study
936 using the San Giacomo granite, *Bulletin of Engineering Geology Environments*, 71, 557-567, 2012.
- 937** Davy, P., Le Goc, R., Darcel, C., Bour, O., de Dreuz, J. R., and Munier, R.: A likely universal model of fracture scaling and its
938 consequence for crustal hydromechanics, *Journal of Geophysical Research: Solid Earth*, 115,
939 <https://doi.org/10.1029/2009JB007043>, 2010.
- 940** DiBiase, R. A., Rossi, M. W., and Neely, A. B.: Fracture density and grain size controls on the relief structure of bedrock
941 landscapes, *Geology*, 48, 399-402, 2018.
- 942** Domokos, G., Jerolmack, D. J., Kun, F., and Torok, J.: Plato's cube and the natural geometry of fragmentation, *Proceedings of the*
943 *National Academy of Sciences*, 117, 18178-18185, 2020.
- 944** Dove, P. M.: Geochemical controls on the kinetics of quartz fracture at subcritical tensile stresses: *Journal of Geophysical Research:*
945 *Solid Earth*, 100, 22349-22359, 1995.
- 946** Eppes, M. C.: Mechanical Weathering: A Conceptual Overview. In: Shroder, J.J.F. (Ed.), *Treatise on Geomorphology*, vol. 3.
947 Elsevier, Academic Press, pp. 30-45, 2022.
- 948** Eppes, M. C. and Griffing, D.: Granular disintegration of marble in nature: A thermal-mechanical origin for a grus and corestone
949 landscape, *Geomorphology*, 117, 170-180, 2010.
- 950** Eppes, M. C. and Keanini, R.: Mechanical weathering and rock erosion by climate-dependent subcritical cracking, *Reviews of*
951 *Geophysics*, 55, 470-508, 2017.
- 952** Eppes, M. C., McFadden, L. D., Wegmann, K. W., and Scuderi, L. A.: Cracks in desert pavement rocks: Further insights into
953 mechanical weathering by directional insolation, *Geomorphology*, 123, 97-108, 2010.
- 954** Eppes, M. C., Magi, B., Scheff, J., Warren, K., Ching, S., and Feng, T.: Warmer, wetter climates accelerate mechanical weathering
955 in field data, independent of stress-loading, *Geophysical Research Letters*, 47, 1-11, 2020.



- 956** Eppes, M. C., Magi, B., Hallet, B., Delmelle, E., Mackenzie-Helnwein, P., Warren, K., and Swami, S.: Deciphering the role of
957 solar-induced thermal stresses in rock weathering, *GSA Bulletin*, 128, 1315-1338, 2016.
- 958** Eppes, M. C., Hancock, G. S., Chen, X., Arey, J., Dewers, T., Huettenmoser, J., Kiessling, S., Moser, F., Tannu, N., Weiserbs, B.,
959 and Whitten, J.: Rates of subcritical cracking and long-term rock erosion, *Geology*, 46, 951-954, 2018.
- 960** Ewan, V. J., West, G. L., and Temporal, J.: Variation in measuring rock joints for tunnelling, *Tunnels and Tunnelling International*,
961 15, 1983.
- 962** Fisher, N. I.: *Statistical Analysis of Circular Data*, Cambridge University Press, Cambridge, England,
963 <https://doi.org/10.1017/CBO9780511564345>, 1993.
- 964** Flinchum, B. A., Holbrook, W. S., Rempe, D., Moon, S., Reibe, C. S., Carr, B. J., Hayes, J. L., St. Clair, J., and Peters, M. P.:
965 Critical zone structure under a granite ridge inferred from drilling and three-dimensional seismic refraction data, *Journal of*
966 *Geophysical Research*, 123, 1317-1343, 2018.
- 967** Girard, L., Gruber, S., Weber, S., and Beutel, J.: Environmental controls of frost cracking revealed through in situ acoustic emission
968 measurements in steep bedrock, *Geophysical Research Letters*, 40, 1748-1753, 10.1002/grl.50384, 2013.
- 969** Gischig, V. S., Moore, J. R., Evans, K. F., Amann, F., and Loew, S.: Thermomechanical forcing of deep rock slope deformation:
970 1. Conceptual study of a simplified slope, *Journal of Geophysical Research*, 116, 10.1029/2011JF002006, 2011.
- 971** Glade, R. C., Shobe, C. M., Anderson, R. S., and Tucker, G. E.: Canyon shape and erosion dynamics governed by channel-hillslope
972 feedbacks, *Geology*, 47, 650-654, 10.1130/G46219.1, 2019.
- 973** Gomez-Heras, M., Smith, B. J., and Fort, R.: Surface temperature differences between minerals in crystalline rocks: Implications
974 for granular disaggregation of granites through thermal fatigue, *Geomorphology*, 78, 236-249, 2006.
- 975** Griffiths, L., Lengliné, O., Heap, M., Baud, P., and Schmittbuhl, J.: Thermal cracking in Westerly Granite monitored using direct
976 wave velocity, coda wave interferometry, and acoustic emissions: *Journal of Geophysical Research: Solid Earth*, 123, 2246-2261,
977 2018.
- 978** Hancock, G. S. and Kirwan, M.: Summit erosion rates deduced from ¹⁰Be: Implications for relief production in the central
979 Appalachians, *Geology*, 35, 89-92, 10.1130/g23147a.1, 2007.
- 980** Handin, J., Hager, R.V., Jr.: Experimental deformation of sedimentary rocks under confining pressure: Tests at high temperature:
981 *AAPG Bull*, 42, 2892-2934, <https://doi.org/10.1306/0BDA5C27-16BD-11D7-8645000102C1865D>, 1958.
- 982** Handin, J., Hager, R.V., Jr.: Experimental deformation of sedimentary rocks Under confining pressure: Tests at room temperature
983 on dry samples: *AAPG Bull*, 41, 1-50, <https://doi.org/10.1306/5CEAE5FB-16BB-11D7-8645000102C1865D>, 1957.
- 984** Handin, J., Hager, R.V., Jr, Friedman, M., Feather, J.N., 1963. Experimental deformation of sedimentary rocks under confining
985 pressure: Pore pressure tests: *AAPG Bull*, 47, 717-755, 1963.
- 986** Heard, H.C.: Effect of large changes in strain rate in the experimental deformation of Yule Marble: *Journal of Geology*,
987 <https://doi.org/10.1086/626892>, 1963.
- 988** Hatir, M. E.: Determining the weathering classification of stone cultural heritage via the analytic hierarchy process and fuzzy
989 inference system, *Journal of Cultural Heritage*, 44, 120-134, <https://doi.org/10.1016/j.culher.2020.02.011>, 2020.
- 990** He, M., Xia, H., Jia, X., Gong, W., Zhao, F., and Liang, K.: Studies on classification, criteria, and control of rockbursts, *Journal of*
991 *Rock Mechanics and Geotechnical Engineering*, 4, 97-114, 10.3724/SP.J.1235.2012.00097, 2012.
- 992** Hennings, P. H., Olson, J. E., and Thompson, L. B.: Combining outcrop data and three-dimensional structural models to
993 characterize fractured reservoirs: An example from Wyoming, *AAPG Bulletin*, 84, 830-849, 10.1306/a967340a-1738-11d7-
994 8645000102c1865d, 2000.
- 995** Hooker, J. N., Laubach, S. E., and Marrett, R.: A universal power-law scaling exponent for fracture apertures in sandstones, *GSA*
996 *Bulletin*, 126, 1340-1362, 10.1130/b30945.1, 2014.



- 997** Isherwood, D. and Street, A.: Biotite-induced grussification of the Boulder Creek Granodiorite, Boulder County, Colorado, GSA
998 Bulletin, 87, 366-370, 10.1130/0016-7606(1976)87<366:Bgotbc>2.0.Co;2, 1976.
- 999** Janio de Castro Lima, J. and Paraguassú, A. B.: Linear thermal expansion of granitic rocks: influence of apparent porosity, grain
1000 size and quartz content, Bulletin of Engineering Geology and the Environment, 63, 215-220, 10.1007/s10064-004-0233-x, 2004.
- 1001** Jenny, H.: Factors of Soil Formation: A System of Quantitative Pedology, McGraw-Hill, New York, New York, 1941.
- 1002** Kobayashi, A. S. and Enetanya, A. N.: Stress intensity factor of a corner crack, Mechanics of Crack Growth, 1976.
- 1003** Krumbein, W. C.: Fundamental attributes of sedimentary particles, University of Iowa Student Engineering Bulletin, 27, 318-331,
1004 1943.
- 1005** Krumbein, W. C. and Sloss, L. L.: Stratigraphy and Sedimentation, W. H. Freeman and Company, San Francisco, California, 1951.
- 1006** La Pointe, P. R.: Derivation of parent fracture population statistics from trace length measurements of fractal fracture populations,
1007 International Journal of Rock Mechanics and Mining Sciences, 39, 381-388, [https://doi.org/10.1016/S1365-1609\(02\)00021-7](https://doi.org/10.1016/S1365-1609(02)00021-7),
1008 2002.
- 1009** Lamp, J. L., Marchant, D. R., Mackay, S. L., and Head, J. W.: Thermal stress weathering and the spalling of Antarctic rocks,
1010 Journal of Geophysical Research: Earth Surface, 122, 3-24, <https://doi.org/10.1002/2016JF003992>, 2017.
- 1011** Leith, K., Moore, J. R., Amann, F., and Loew, S.: In situ stress control on microcrack generation and macroscopic extensional
1012 fracture in exhuming bedrock, Journal of Geophysical Research, 119, 1-22, 2014.
- 1013** Leone, J. D., Holbrook, W. S., Reibe, C. S., Chorover, J., Ferre, T. P. A., Carr, B. J., and Callahan, R. P.: Strong slope-aspect
1014 control of regolith thickness by bedrock foliation, Earth Surface Processes and Landforms, 45, 2998-3010, 2020.
- 1015** Long, J., Jones, R., Daniels, S., Gilment, S., Oxlade, D., and Wilkinson, M.: PS Reducting Uncertainty in Fracture Modelling:
1016 Assessing user bias in interpretations from satellite imagery, AAPG 2019 Annual Convention & Exhibition, San Antonio, TX,
1017 2019.
- 1018** Macholdt, D. S., Al-Amri, A. M., Tuffaha, H. T., Jochum, K. P., and Andreae, M. O.: Growth of desert varnish on petroglyphs
1019 from Jubbah and Shuwaymis, Ha'il region, Saudi Arabia, The Holocene, 28, 1495-1511, 2018.
- 1020** Maffucci, R., Bigi, S., Corrado, S., Chiodi, A., Di Paolo, L., Giordano, G., and Invernizzi, C.: Quality assessment of reservoirs by
1021 means of outcrop data and “discrete fracture network” models: The case history of Rosario de La Frontera (NW Argentina)
1022 geothermal system, Tectonophysics, 647-648, 112-131, <https://doi.org/10.1016/j.tecto.2015.02.016>, 2015.
- 1023** Mardia, K. V. and Jupp, P. E.: Directional Statistics, Academic Press Inc., London, England, 1972.
- 1024** Marshall, J., Clyne, J., Eppes, M. C., and Dawson, T.: Barking up the wrong tree? Tree root tapping, subcritical cracking, and
1025 potential influence on bedrock porosity, 2021.
- 1026** Martel, S. J.: Effect of topographic curvature on near-surface stresses and application to sheeting joints, Geophysical Research
1027 Letters, 33, 2006.
- 1028** Martel, S. J.: Mechanics of curved surfaces, with application to surface-parallel cracks, Geophysical Research Letters, 38, 2011.
- 1029** Martel, S. J.: Progress in understanding sheeting joints over the past two centuries, Journal of Structural Geology, 94, 68-86, 2017.
- 1030** Matsuoka, N. and Murton, J.: Frost weathering: Recent advances and future directions, Permafrost and Periglacial Processes, 19,
1031 195-210, 10.1002/ppp.620, 2008.
- 1032** McAuliffe, J.R., McFadden, L.D., Persico, L.P. and Rittenour, T.M.: Climate and Vegetation Change, Hillslope Soil Erosion, and
1033 the Complex Nature of Late Quaternary Environmental Transitions, Eastern Mojave Desert, USA, Quaternary, 5, 43, 2022.
- 1034** McFadden, L. D., Ritter, J. B., and Wells, S. G.: Use of multiparameter relative-age methods for age estimation and correlation of
1035 alluvial fan surfaces on a desert piedmont, eastern Mojave Desert, California, Quaternary Research, 32, 276-290, 1989.



- 1036** McFadden, L. D., Eppes, M. C., Gillespie, A. R., and Hallet, B.: Physical weathering in arid landscapes due to diurnal variation in the direction of solar heating, *GSA Bulletin*, 117, 161-173, 2005.
- 1037**
- 1038** Milad, B. and Slatt, R.: Outcrop to subsurface reservoir characterization of the Mississippian Sycamore/Meramec play in the SCOOP Area, Arbuckle Mountains, Oklahoma, USA, SPE/AAPG/SEG Unconventional Resources Technology Conference, 10.15530/urtec-2019-991,
- 1039**
- 1040**
- 1041** Mogi, K.: Fracture and flow of rocks under high triaxial compression: *Journal of Geophysical Research*, 76, 1255–1269, <https://doi-org.nmt.idm.oclc.org/10.1029/JB076i005p01255>, 1971.
- 1042**
- 1043** Mogi, K.: Effect of the intermediate principal stress on rock failure: *Journal of Geophysical Research*, 72, 5117–5131, 1967.
- 1044** Molaro, J. L., Byrne, S., and Le, J.-L.: Thermally induced stresses in boulders on airless body surfaces, and implications for rock breakdown, *Icarus*, 294, 247-261, 2017.
- 1045**
- 1046** Molaro, J. L., Hergenrother, C. W., Chesley, S. R., Walsh, K. J., Hanna, R. D., Haberle, C. W., Schwartz, S. R., Ballouz, R.-L., Bottke, W. F., Campins, H. J., and Lauretta, D. S.: Thermal fatigue as a driving mechanism for activity on asteroid Bennu, *Journal of Geophysical Research*, 125, 1-24, 10.1029/2019JE006325, 2020.
- 1047**
- 1048**
- 1049** Molnar, P.: Interactions among topographically induced elastic stress, static fatigue, and valley incision, *Journal of Geophysical Research*, 109, 1-9, 10.1029/2003JF000097, 2004.
- 1050**
- 1051** Moon, S., Perron, J. T., Martel, S. J., Goodfellow, B. W., Ivars, D. M., Hall, A., Heyman, J., Munier, R., Naslund, J., Simeonov, A., and Stroeven, A. P.: Present-day stress field influences bedrock fracture openness deep into the subsurface, *Geophysical Research Letters*, 47, 1-10, 2020.
- 1052**
- 1053**
- 1054** Moser, F.: Spatial and temporal variance in rock dome exfoliation and weathering near Twain Harte, California, USA, *Geography and Earth Sciences*, The University of North Carolina Charlotte, ProQuest, 2017.
- 1055**
- 1056** Mushkin, A., Sagy, A., Trabelci, E., Amit, R., and Porat, N.: Measure the time and scale-dependency of subaerial rock weathering rates over geologic time scales with ground-based lidar, *Geology*, 42, 1063-1066, 2014.
- 1057**
- 1058** Nara, Y. and Kaneko, K.: Sub-critical crack growth in anisotropic rock, *International Journal of Rock Mechanics and Mining Sciences*, 43, 437-453, <https://doi.org/10.1016/j.ijrmms.2005.07.008>, 2006.
- 1059**
- 1060** Nara, Y., Kashiwaya, K., Nishida, Y., and Ii, T.: Influence of surrounding environment on subcritical crack growth in marble, *Tectonophysics*, 706-707, 116-128, 2017.
- 1061**
- 1062** Neely, A. B., DiBiase, R. A., Corbett, L. B., Bierman, P. R., and Caffee, M. W.: Bedrock fracture density controls on hillslope erodibility in steep, rocky landscapes with patchy soil cover, southern California, USA, *Earth and Planetary Science Letters*, 522, 186-197, <https://doi.org/10.1016/j.epsl.2019.06.011>, 2019.
- 1063**
- 1064**
- 1065** Novitsky, C. G., Holbrook, W. S., Carr, B. J., Pasquet, S., Okaya, D., and Flinchum, B. A.: Mapping inherited fractures in the critical zone using seismic anisotropy from circular surveys, *Geophysical Research Letters*, 45, 3126-3135, <https://doi.org/10.1002/2017GL075976>, 2018.
- 1066**
- 1067**
- 1068** Ollier, C. D.: *Weathering*, 2nd, Longman, London, England, 1984.
- 1069** Olsen, T., Borella, J., and Stahl, T.: Clast transport history influences Schmidt hammer rebound values, *Earth Surface Processes and Landforms*, 45, 1392-1400, <https://doi.org/10.1002/esp.4809>, 2020.
- 1070**
- 1071** Olson, J. E.: Predicting fracture swarms - the influence of subcritical crack growth and the crack-tip process zone on joint spacing in rock, *Geological Society of London Special Publications*, 231, 73-87, 2004.
- 1072**
- 1073** Ortega, O. and Marrett, R.: Prediction of macrofracture properties using microfracture information, Mesaverde Group sandstones, San Juan basin, New Mexico, *Journal of Structural Geology*, 22, 571-588, [https://doi.org/10.1016/S0191-8141\(99\)00186-8](https://doi.org/10.1016/S0191-8141(99)00186-8), 2000.
- 1074**
- 1075** Ortega, O. J., Marrett, R. A., and Laubach, S. E.: A scale-independent approach to fracture intensity and average spacing measurement, *AAPG Bulletin*, 90, 193-208, 10.1306/08250505059, 2006.
- 1076**



- 1077** Paris, P. C. and Erdogan, F.: A critical analysis of crack propagation laws, *Journal of Basic Engineering*, 85, 528-533,
1078 <https://doi.org/10.1115/1.3656900>, 1963.
- 1079** Persico, L. P., L. D. McFadden, J. R. McAuliffe, T. M. Rittenour, T. E. Stahlecker, S. B. Dunn, and S. A. T. Brody: Late Quaternary
1080 geochronologic record of soil formation and erosion: Effects of climate change on Mojave Desert hillslopes (Nevada, USA),
1081 *Geology*, 50, 54-59, 2021.
- 1082** Ponti, S., Pezza, M., and Guglielmin, M.: The development of Antarctic tafoni: Relations between differential weathering rates
1083 and spatial distribution of thermal events, salts concentration, and mineralogy, *Geomorphology*, 373, 2021.
- 1084** Ramacharan, A., Hengl, T., Nauman, T., Brungard, C., Waltman, S., Wills, S., and Thompson, J.: Soil property and class maps of
1085 the conterminous United States at 100-meter spatial resolution, *Soil Science Society of America Journal*, 82, 186-201, 2018.
- 1086** Ramulu, M., Chakraborty, A. K., and Sitharam, T. G.: Damage assessment of basaltic rock mass due to repeated blasting in a
1087 railway tunnelling project – A case study, *Tunnelling and Underground Space Technology*, 24, 208-221,
1088 <https://doi.org/10.1016/j.tust.2008.08.002>, 2009.
- 1089** Rasmussen, M., Eppes, M. C., and Berberich, S.: Untangling the impacts of climate, lithology, and time on rock cracking rates and
1090 morphology in arid and semi-arid Eastern California, *AGU Fall Meeting*, New Orleans, LA, 2021.
- 1091** Ravaji, B., Lagoa, V. A., Delbo, M., and Wilkerson, J.: Unraveling the mechanics of thermal stress weathering: rate-effects, size-
1092 effects, and scaling laws, *Journal of Geophysical Research: Planets*, 124, 3304-3328, 2019.
- 1093** Riebe, C. S., Callahan, R. P., Granke, S. B.-M., Carr, B. J., Hayes, J. L., Schell, M. S., and Sklar, L. S.: Anisovolumetric weathering
1094 in granitic saprolite controlled by climate and erosion rate, *Geology*, 1-5, [10.1130/G48191.1](https://doi.org/10.1130/G48191.1), 2021.
- 1095** Røyne, A., Jamtveit, B., Mathiesen, J., and Malthe-Sørenssen, A.: Controls on rock weathering rates by reaction-induced
1096 hierarchical fracturing, *Earth and Planetary Science Letters*, 275, 364-369, <https://doi.org/10.1016/j.epsl.2008.08.035>, 2008.
- 1097** Scarciglia, F., Saporito, N., La Russa, M. F., Le Pera, E., Macchione, M., Puntillo, D., Crisci, G. M., and Pezzino, A.: Role of
1098 lichens in weathering of granodiorite in the Sila uplands (Calabria, southern Italy), *Sedimentary Geology*, 280, 119-134, 2012.
- 1099** Schoeneberger, P. J., Wysocki, D. A., and Benham, E. C.: *Field Book for Describing and Sampling Soils: Version 3.0*, Natural
1100 Resources Conservation Service, National Soil Survey Center, Lincoln, Nebraska, 2012.
- 1101** Schultz, R. A.: *Geologic Fracture Mechanics*, Cambridge University Press, Cambridge, England, DOI: 10.1017/9781316996737,
1102 2019.
- 1103** Shaanan, U., Mushkin, A., Rasmussen, M., Sagy, A., Morad, D. and Eppes, M.c.: Zonation within incipient cracks in boulders and
1104 indications for their subcritical propagation over geologic time scales, *Geological Society of America Abstracts with Programs*,
1105 PRF2022 Penrose Conference, <https://doi.org/10.1130/abs/2022PR-376049>, 2022.
- 1106** Sharifigaliuk, H., Mahmood, S. M., Ahmad, M., and Rezaee, R.: Use of outcrop as substitute for subsurface shale: Current
1107 understanding of similarities, discrepancies, and associated challenges, *Energy & Fuels*, 35, <https://doi.org/9151-9164>,
1108 10.1021/acs.energyfuels.1c00598, 2021.
- 1109** Shi, J.: *Study of thermal stresses in rocks due to diurnal solar exposure*, Civil Engineering, University of Washington, 58 pp., 2011.
- 1110** Shobe, C. M., Hancock, G. S., Eppes, M. C., and Small, E. E.: Field evidence for the influence of weathering on rock erodibility
1111 and channel form in bedrock rivers, *Earth Surface Processes and Landforms*, 42, 1997-2012, 2017.
- 1112** Snowdon, A. P., Normani, S. D., and Sykes, J. F.: Analysis of crystalline rock permeability versus depth in a Canadian Precambrian
1113 rock setting, *Journal of Geophysical Research: Solid Earth*, 126, e2020JB020998, <https://doi.org/10.1029/2020JB020998>, 2021.
- 1114** Sousa, L. M. O.: Evaluation of joints in granitic outcrops for dimension stone exploitation, *Quarterly Journal of Engineering*
1115 *Geology and Hydrogeology*, 43, 85-94, <https://doi.org/10.1144/1470-9236/08-076>, 2010.
- 1116** St. Clair, J., Moon, S., Holbrook, W. S., Perron, J. T., Riebe, C. S., Martel, S. J., Carr, B., Harman, C., Singha, K., and Richter, D.
1117 D.: Geophysical imaging reveals topographic stress control of bedrock weathering, *Geomorphology*, 350, 534-538, 2015.



- 1118** Staff, S. S.: Soil Taxonomy: A basic system of soil classification for making and interpreting soil surveys, 1999.
- 1119** Terry, R. D. and Chilingar, G. V.: Summary of "Concerning some additional aids in studying sedimentary formations," by MS
1120 Shvetsov, Journal of Sedimentary Research, 25, 229-234, 1955.
- 1121** Turner, J., Griggs, D., Heard, H.C.: Experimental deformation of calcite crystals: Bulletin of the Geological Society of America,
1122 86, 883–934, 1954.
- 1123** Ukar, E., Laubach, S. E., and Hooker, J. N.: Outcrops as guides to subsurface natural fractures: Example from the Nikanassin
1124 Formation tight-gas sandstone, Grande Cache, Alberta foothills, Canada, Marine and Petroleum Geology, 103, 255-275,
1125 <https://doi.org/10.1016/j.marpetgeo.2019.01.039>, 2019.
- 1126** Ulusay, R., Hudson, J.A.: The Complete ISRM Suggested Methods for Rock Characterization, Testing and Monitoring: 1974-
1127 2006. ISRM, Ankara, Turkey, 2007.
- 1128** Vázquez, P., Shushakova, V., and Gómez-Heras, M.: Influence of mineralogy on granite decay induced by temperature increase:
1129 Experimental observations and stress simulation, Engineering Geology, 189, 58-67, 2015.
- 1130** Wang, H., Bonner, B., Carlson, S., Kowallis, B., and Heard, H.: Thermal stress cracking in granite: Journal of Geophysical
1131 Research: Solid Earth (1978–2012), 94, 1745-1758, 1989.
- 1132** Watkins, H., Bond, C. E., Healy, D., and Butler, R. W. H.: Appraisal of fracture sampling methods and a new workflow to
1133 characterise heterogeneous fracture networks at outcrop, Journal of Structural Geology, 72, 67-82,
1134 <https://doi.org/10.1016/j.jsg.2015.02.001>, 2015.
- 1135** Weiserbs, B. I.: The morphology and history of exfoliation on rock domes in the Southeastern United States, Geography and Earth
1136 Sciences, The University of North Carolina Charlotte, ProQuest, 2017.
- 1137** Weiss, M.: Techniques for estimating fracture size: A comparison of methods, International Journal of Rock Mechanics and Mining
1138 Sciences, 45, 460-466, <https://doi.org/10.1016/j.ijrmms.2007.07.010>, 2008.
- 1139** Wenk, H.-R.: Some roots of experimental rock deformation: Bulletin Minéralogie, 102, 195–202,
1140 <https://doi.org/10.3406/bulmi.1979.7277>, 1979.
- 1141** West, N., Kirby, E., Bierman, P. R., and Clarke, B. A.: Aspect-dependent variations in regolith creep revealed by meteoric ¹⁰Be,
1142 Geology, 42, 507-510, 10.1130/g35357.1, 2014.
- 1143** Wohl, E. E.: The effect of bedrock jointing on the formation of straths in the Cache la Poudre River drainage, Colorado Front
1144 Range, Journal of Geophysical Research: Earth Surface, 113, <https://doi.org/10.1029/2007JF000817>, 2008.
- 1145** Wolman, M. G.: A method of sampling coarse river-bed material, Eos, Transactions American Geophysical Union, 35, 951-956,
1146 <https://doi.org/10.1029/TR035i006p00951>, 1954.
- 1147** Wu, H. and Pollard, D. D.: An experimental study of the relationship between joint spacing and layer thickness, Journal of
1148 Structural Geology, 17, 887-905, [https://doi.org/10.1016/0191-8141\(94\)00099-L](https://doi.org/10.1016/0191-8141(94)00099-L), 1995.
- 1149** Zeeb, C., Gomez-Rivas, E., Bons, P. D., and Blum, P.: Evaluation of sampling methods for fracture network characterization using
1150 outcrops, AAPG Bulletin, 97, 1545-1566, 2013.
- 1151** Zhang, C., Hu, X., Wu, Z., and Li, Q.: Influence of grain size on granite strength and toughness with reliability specified by normal
1152 distribution, Theoretical and Applied Fracture Mechanics, 96, 534-544, <https://doi.org/10.1016/j.tafmec.2018.07.001>, 2018.
- 1153** Zhou, W., Shi, G., Wang, J., Liu, J., Xu, N., and Liu, P.: The influence of bedding planes on tensile fracture propagation in shale
1154 and tight sandstone, Rock Mechanics and Rock Engineering, 55, 1111-1124, 10.1007/s00603-021-02742-2, 2022.
- 1155**

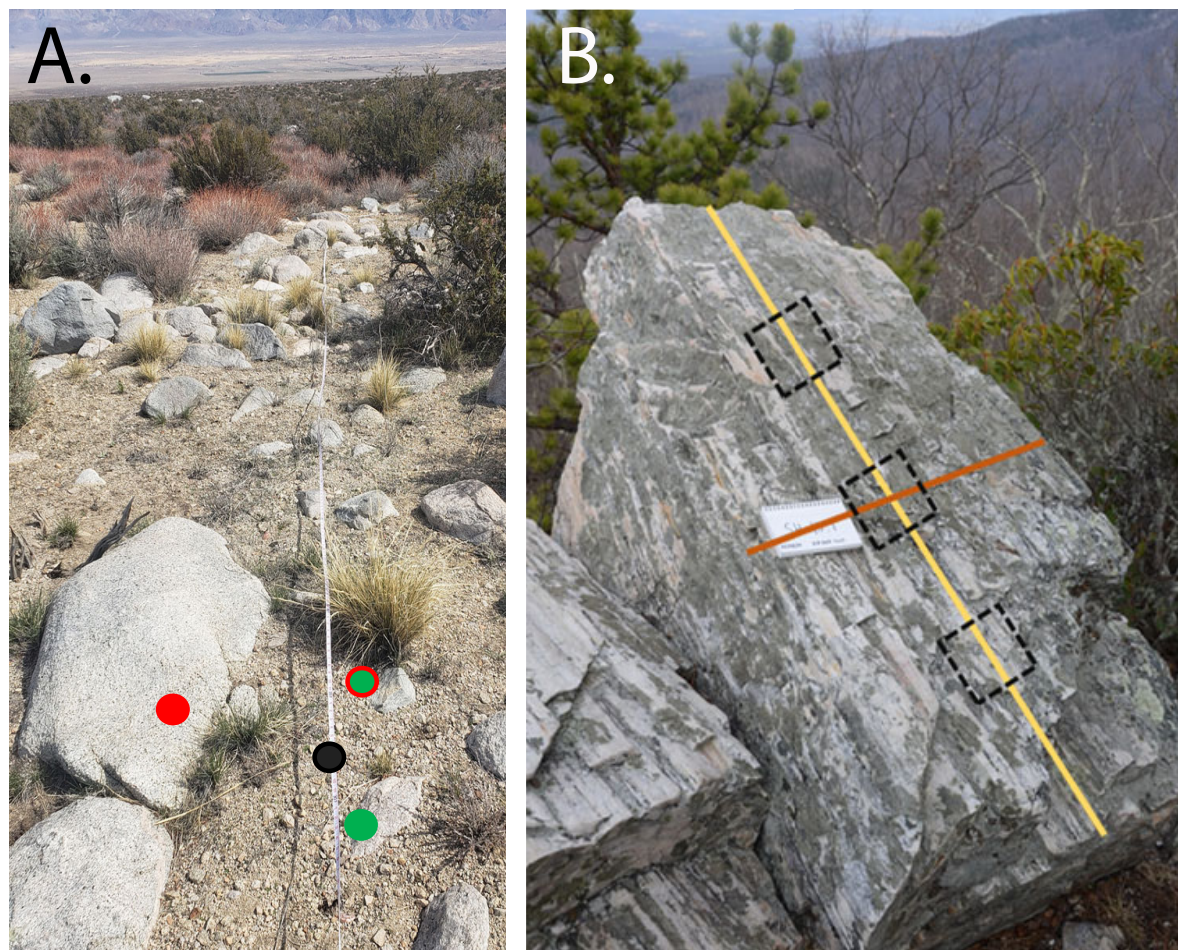


Fig. 1



Fig. 2

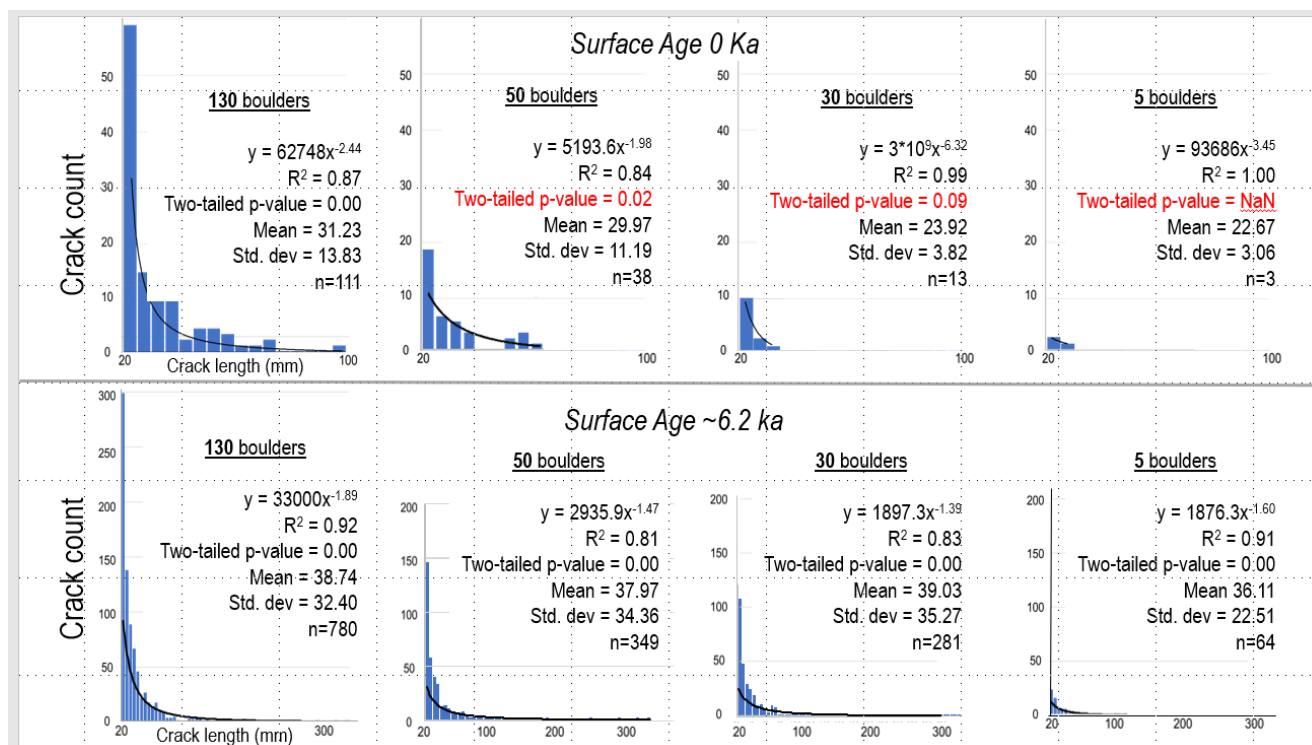


Fig. 3



Name(s) & Date:		Criteria for Clast/Outcrop selection:		Relevant Cl, O, R, P, T, T observations:																				
Site Name:				Vegetation-type & percent of each:																				
GPS Coordinates:				open ground cover (%):																				
Orientation conventions:		Portion observed (eg. All exposed, north face only, etc.):		Surface Slope:																				
Declination:				Other:																				
ID & Rock Type	Avg. Grain Size (mm)	spheri- city/ round- ness	Mineralogy	Length (cm)	Width (cm)	Height (cm)	Exposure	Cracks cm	GD & Pit	Lichen	Varnish	Fabric Type	Fabric Strike (°)	Fabric Dip (°)	Crack ID	Crack Parallel to	Mid Crack Width (mm)	Crack Max Width (mm)	Crack Length (mm)	Crack Strike (°)	Crack Dip (°)	Sheet Ht. (mm)	Weathering Index	Notes
							0123	012345	gp	012345	012345	F8BVO				SFL							12345	
							0123	012345	gp	012345	012345	F8BVO				SFL							12345	
							0123	012345	gp	012345	012345	F8BVO				SFL							12345	
							0123	012345	gp	012345	012345	F8BVO				SFL							12345	
							0123	012345	gp	012345	012345	F8BVO				SFL							12345	
							0123	012345	gp	012345	012345	F8BVO				SFL							12345	
							0123	012345	gp	012345	012345	F8BVO				SFL							12345	
							0123	012345	gp	012345	012345	F8BVO				SFL							12345	
							0123	012345	gp	012345	012345	F8BVO				SFL							12345	
							0123	012345	gp	012345	012345	F8BVO				SFL							12345	
							0123	012345	gp	012345	012345	F8BVO				SFL							12345	
							0123	012345	gp	012345	012345	F8BVO				SFL							12345	
							0123	012345	gp	012345	012345	F8BVO				SFL							12345	
							0123	012345	gp	012345	012345	F8BVO				SFL							12345	
							0123	012345	gp	012345	012345	F8BVO				SFL							12345	
							0123	012345	gp	012345	012345	F8BVO				SFL							12345	
							0123	012345	gp	012345	012345	F8BVO				SFL							12345	
							0123	012345	gp	012345	012345	F8BVO				SFL							12345	
							0123	012345	gp	012345	012345	F8BVO				SFL							12345	
							0123	012345	gp	012345	012345	F8BVO				SFL							12345	
							0123	012345	gp	012345	012345	F8BVO				SFL							12345	
							0123	012345	gp	012345	012345	F8BVO				SFL							12345	
							0123	012345	gp	012345	012345	F8BVO				SFL							12345	
							0123	012345	gp	012345	012345	F8BVO				SFL							12345	
							0123	012345	gp	012345	012345	F8BVO				SFL							12345	
							0123	012345	gp	012345	012345	F8BVO				SFL							12345	
							0123	012345	gp	012345	012345	F8BVO				SFL							12345	
							0123	012345	gp	012345	012345	F8BVO				SFL							12345	
							0123	012345	gp	012345	012345	F8BVO				SFL							12345	
							0123	012345	gp	012345	012345	F8BVO				SFL							12345	
							0123	012345	gp	012345	012345	F8BVO				SFL							12345	
							0123	012345	gp	012345	012345	F8BVO				SFL							12345	
							0123	012345	gp	012345	012345	F8BVO				SFL							12345	
							0123	012345	gp	012345	012345	F8BVO				SFL							12345	
							0123	012345	gp	012345	012345	F8BVO				SFL							12345	
							0123	012345	gp	012345	012345	F8BVO				SFL							12345	
							0123	012345	gp	012345	012345	F8BVO				SFL							12345	
							0123	012345	gp	012345	012345	F8BVO				SFL							12345	
							0123	012345	gp	012345	012345	F8BVO				SFL							12345	
							0123	012345	gp	012345	012345	F8BVO				SFL							12345	
							0123	012345	gp	012345	012345	F8BVO				SFL							12345	
							0123	012345	gp	012345	012345	F8BVO				SFL							12345	
							0123	012345	gp	012345	012345	F8BVO				SFL							12345	
							0123	012345	gp	012345	012345	F8BVO				SFL							12345	
							0123	012345	gp	012345	012345	F8BVO				SFL							12345	
							0123	012345	gp	012345	012345	F8BVO				SFL							12345	
							0123	012345	gp	012345	012345	F8BVO				SFL							12345	
							0123	012345	gp	012345	012345	F8BVO				SFL							12345	
							0123	012345	gp	012345	012345	F8BVO				SFL							12345	
							0123	012345	gp	012345	012345	F8BVO				SFL							12345	
							0123	012345	gp	012345	012345	F8BVO				SFL							12345	
							0123	012345	gp	012345	012345	F8BVO				SFL							12345	
							0123	012345	gp	012345	012345	F8BVO				SFL							12345	
							0123	012345	gp	012345	012345	F8BVO				SFL							12345	
							0123	012345	gp	012345	012345	F8BVO				SFL							12345	
							0123	012345	gp	012345	012345	F8BVO				SFL							12345	
							0123	012345	gp	012345	012345	F8BVO				SFL							12345	
							0123	012345	gp	012345	012345	F8BVO				SFL							12345	
							0123	012345	gp	012345	012345	F8BVO				SFL							12345	
							0123	012345	gp	012345	012345	F8BVO				SFL							12345	
							0123	012345	gp	012345	012345	F8BVO				SFL							12345	
							0123	012345	gp	012345	012345	F8BVO				SFL							12345	
							0123	012345	gp	012345	012345	F8BVO				SFL							12345	
							0123	012345	gp	012345	012345	F8BVO				SFL							12345	
							0123	012345	gp	012345	012345	F8BVO				SFL							12345	
							0123	012345	gp	012345	012345	F8BVO				SFL							12345	
							0123	012345	gp	012345	012345	F8BVO				SFL							12345	
							0123	012345	gp	012345	012345	F8BVO				SFL							12345	
							0123	012345	gp	012345	012345	F8BVO				SFL							12345	
							0123	012345	gp	012345	012345	F8BVO				SFL							12345	
							0123	012345	gp	012345	012345	F8BVO				SFL							12345	
							0123	012345	gp	012345	012345	F8BVO				SFL							12345	
							0123	012345	gp	012345	012345	F8BVO				SFL							12345	
							0123	012345	gp	012345	012345	F8BVO				SFL							12345	
							0123	012345	gp	012345	012345	F8BVO				SFL							12345	
							0123	012345	gp	012345	012345	F8BVO				SFL							12345	
							0123	012345	gp	012345	012345	F8BVO				SFL							12345	
							0123	012345	gp	012345	012345	F8BVO				SFL							12345	
							0123	012345	gp	012345	012345	F8BVO				SFL							12345	
							0123	012345	gp	012345	012345	F8BVO				SFL							12345	
							0123	012																

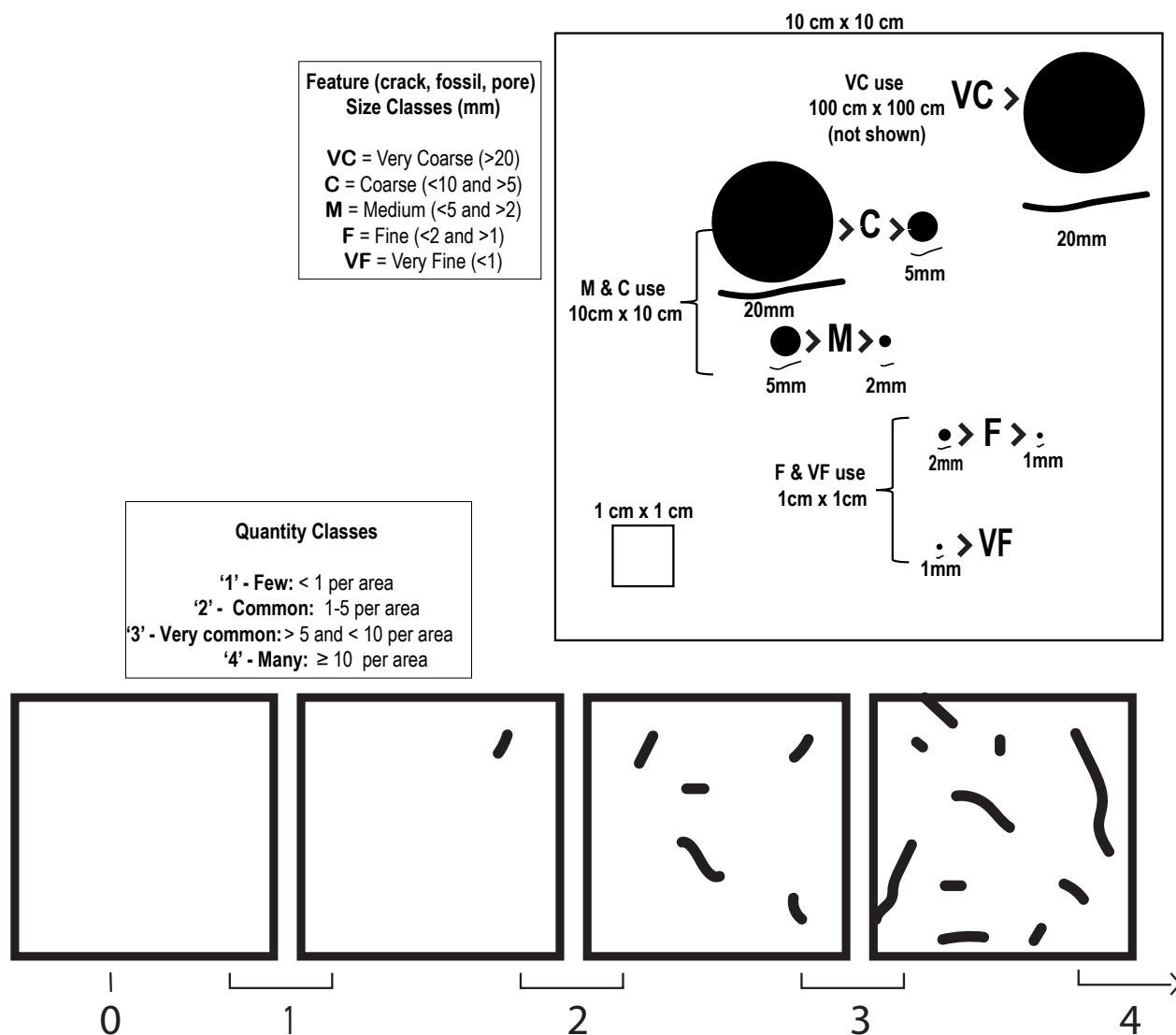


Fig. 5

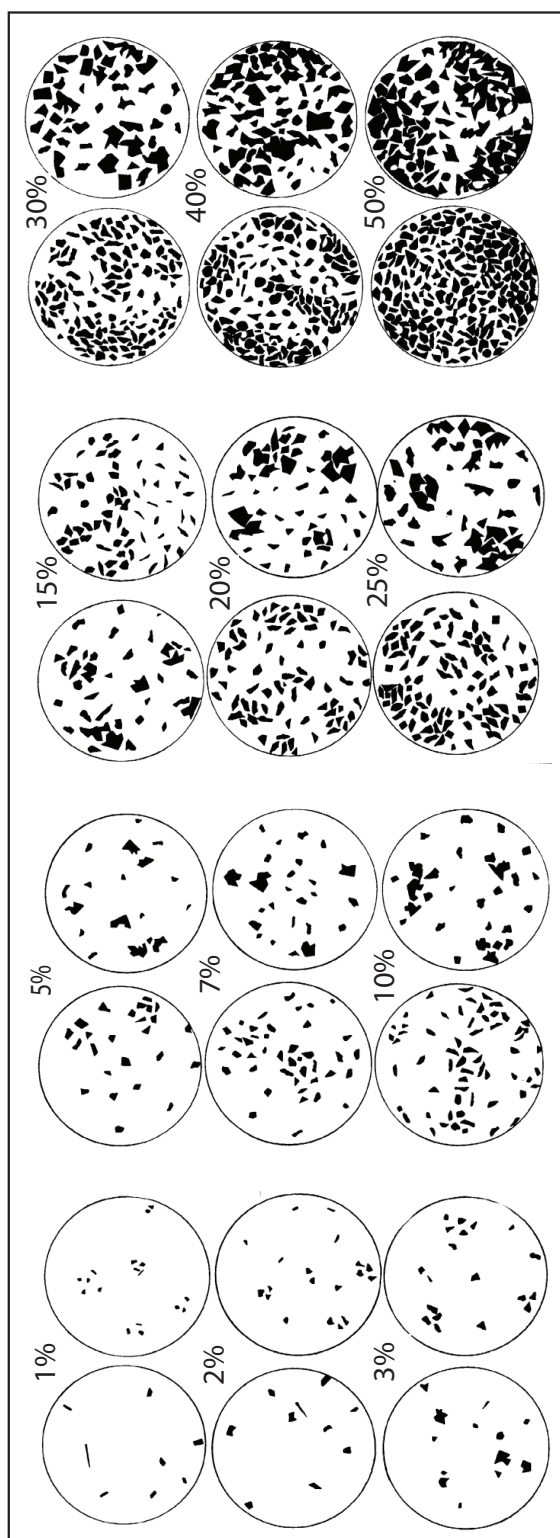


Fig. 6

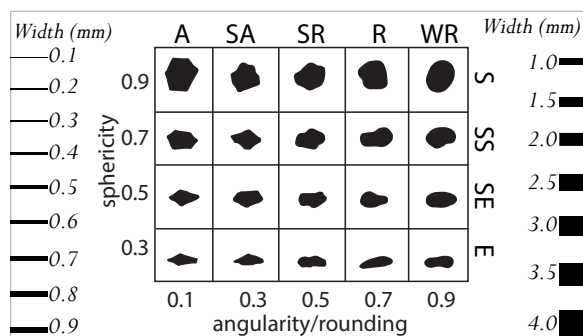


Fig. 7

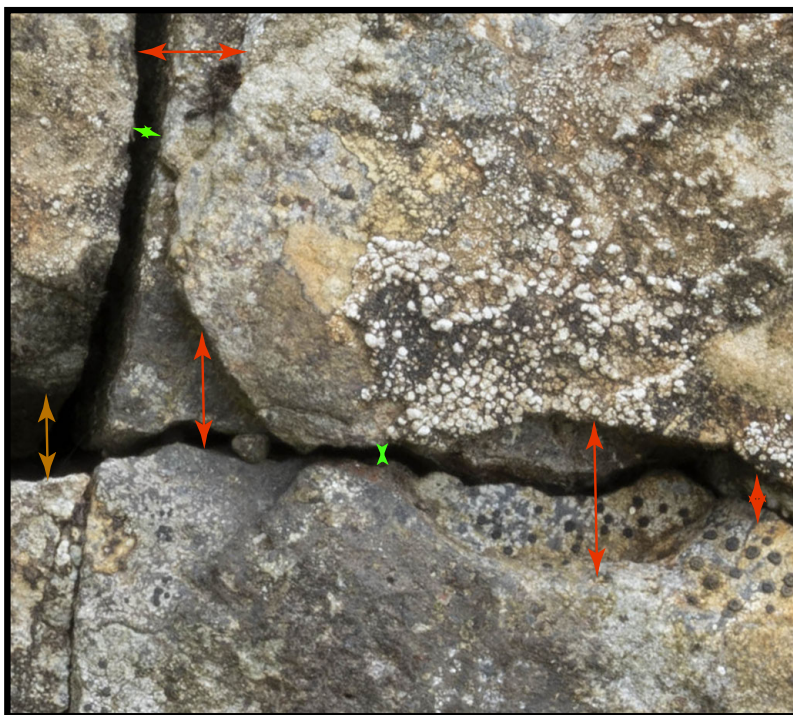


Fig. 8

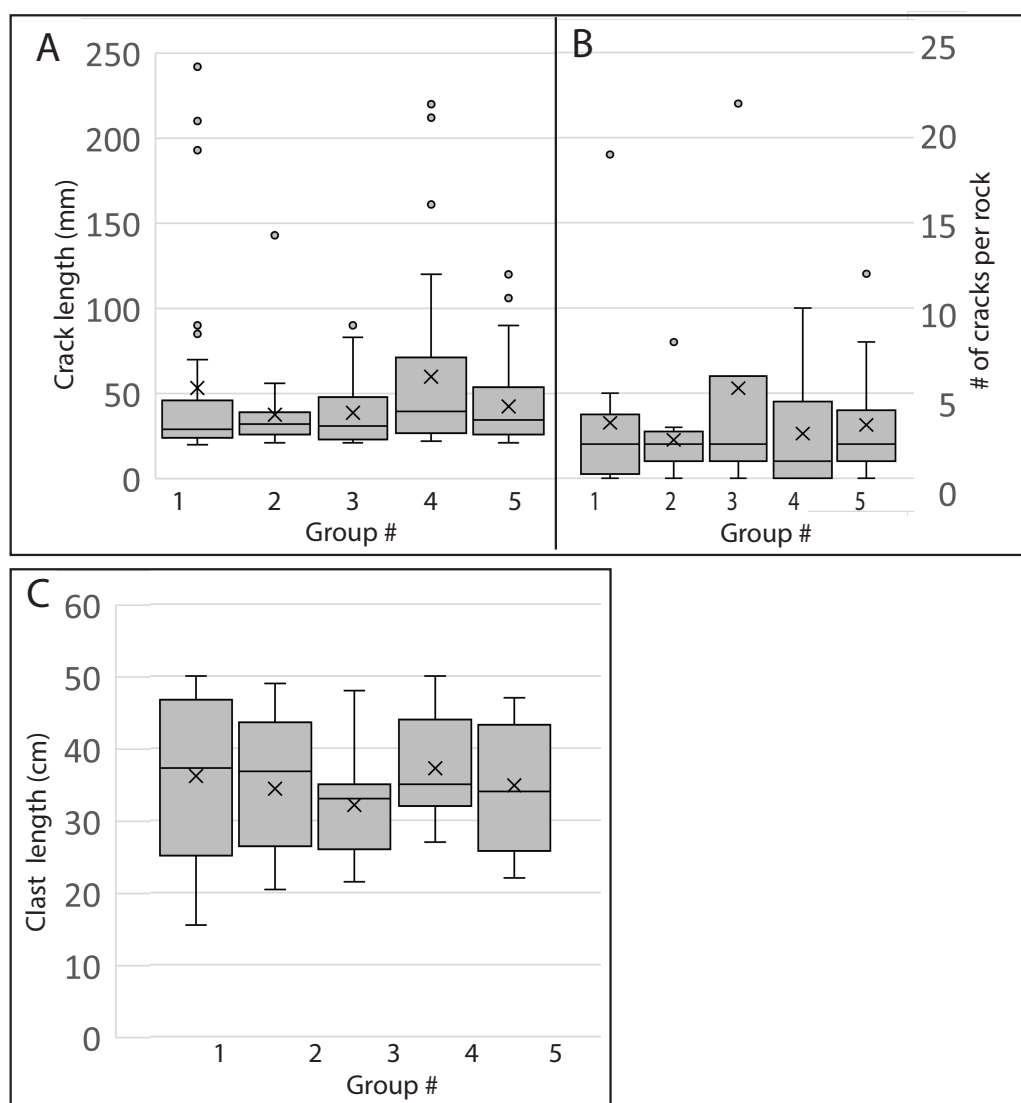


Fig 9.